Nasal Drug Delivery Using Mucoadhesive pH-Sensitive Polymers and β-Sitosterol β-D-Glucoside

Koji Nakamura

INDEX

LIST OF PUBLICATION

(1) Uptake and release of budesonide from mucoadhesive, pH-sensitive copolymers and their application to nasal delivery: Kouji Nakamura, Yoshie Maitani, Anthony M. Lowman, Kozo Takayama, Nicholas A. Peppas, Tsuneji Nagai. *J Controlled Release*, 1999, 61, 329-335. <presented in *Chapter I* of this dissertation>.

(2) The enhancing effect of soybean-derived sterylglucoside and β-sitosterol β-D-glucoside on nasal absorption in rabbits. Yoshie Maitani, Kouji Nakamura, Hiroshi Suenaga, Katsuo Kamata, Kozo Takayama, Tsuneji Nagai. *Int J Pharm*, 2000, 200, 17-36. <presented in *Chapter II* of this dissertation>.

(3) The enhancing effect of nasal absorption of FITC-dextran 4,400 by β-sitosterol β-D-glucoside in rabbits. Kouji Nakamura, Yoshie Maitani, Kozo Takayama. *J Controlled Release,* in press. <presented in *Chapter II* of this dissertation>.

(4) Enhancing effect of FITC-dextran absorption via nasal mucosa by nanoparticle based on β-sitosterol β-D-glucoside and its aglycon. Kouji Nakamura, Yoshie Maitani, Kozo Takayama. *S.T.P. Pharma Sci.*, in press. <presented in *Chapter III* of this dissertation>.

Abbreviations

AUC	area under the drug concentration-curve
C10	sodium caprate
$[Ca^{2+}]i$	intracellular calcium ion
Cmax	maximum blood concentration
DMSO	dimethyl sulphoxide
D-PBS	dulbecco's phosphate buffered saline
EDTA	ethylenediamine-tetraacetate
Ef	enhancing factor
F	bioavailability
FD-4	fluorescent isothiocianate dextran 4,400
Isc	short-circuit current
Ka	absorption constant rate
MRT	mean residence time
Nanoparticles	NP
Papp	apparent permeability coefficients
PEG	polyethylene glycol
PBS	phosphate-buffered saline, pH 7.4
PD	potential difference
PMAA	polymethacrylic acid
P(MAA-g-EG)	hydrogel based poly(methacrylic acid) grafted with poly(ethylene glycol)
SG	soybean-derived sterol glucoside
Sit	β-sitosterol

Sit-G	β-sitosterol β-D-glucoside
SP	powder sieved with 200 mesh (75 μm)
SS	soybean-derived sterol
TEER	transepithelial resistance
Tmax	the time reached at Cmax
Tris-buffer	trisaminomethane-HCl buffer

GENERAL INTRODUCTION

Oral drug delivery has been known for decades as the most widely utilized route of administration among all the routes that have been explored for the systemic delivery of drugs. However, when orally administered, drugs were subjected to extensive metabolism in the liver, termed as the hepatic first-pass metabolism [1]. The consequence of hepatic first-pass metabolism induces the low bioavailability, not reaching to sufficient levels of drug in plasma for therapy.

The nasal drug delivery offers many advantages that include the avoidance of the hepatic first-pass metabolism, rapid absorption due to a highly permeable tissue and ease of administration. Currently, two classes of nasally delivered therapeutics are on the market. The first class includes local anti-inflammatory. The second one includes a few peptide drugs such as buserelin, desmopressin and calcitonin.

The nasal cavity has a large surface area for absorption of drugs due to the fact that the nasal cavity is covered with numerous microvilli and the presence of turbinate structures. Furthermore, the subepithelial layer is highly vascularized with the additional benefit of the venous blood passing directly into the systemic circulation thereby avoiding the first-pass metabolism.

Airway epithelium in the nose consists of four cell types. These are nonciliated columnar cells, goblet cells, basal cells, and ciliated columnar cells (*Figure 1*). The goblet cells, together with the nasal glands in the respiratory pathways, produce the mucous secretion. The mucosal surface is covered by a layer of secretions, which contain mucous glycoproteins, imunoglobulins, albumin, lysozome, and other substances. Basically, there are two transport pathways potentially involved drug

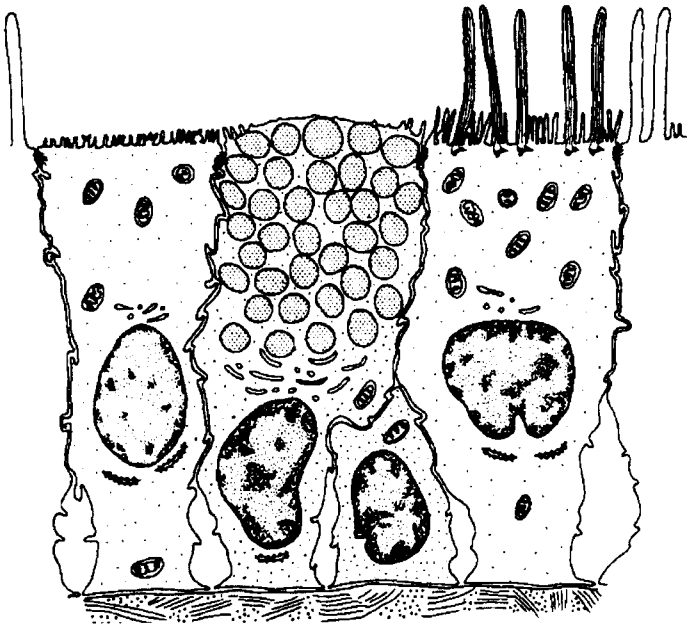

Figure 1. The structure of nasal epithelium
I. nonciliated columnar cell with microvilli,
II. goblet cell, III. basal cell, IV. ciliated columnar cell

permeation across epithelial membranes; the paracellular and the transcellular pathway (*Figure 2*). Mainly, the hydrophilic drug passed between cells (paracellular pathway), and this pathway was restricted by tight junctions located between mucosal membranes. The hydrophilic drug permeability is dependent on the molecular weight [2] although the molecules with less than 1,000 Da are relatively permeated across mucosal membrane [3,4]. On the other hand, transcellular pathway means that hydrophobic drug traverses inside cells. Large hydrophilic drugs such as peptide and protein are not easily absorbed by the nasal route. Most peptide and protein show the low bioavailabilities when administered nasally. The main reasons for such a low degree of absorption of these molecules has reasonably been suggested to be their hydrophilic nature, their large molecular size and physiological factors such as enzymatic degradation of the molecules in the nasal cavity and their movement away from the

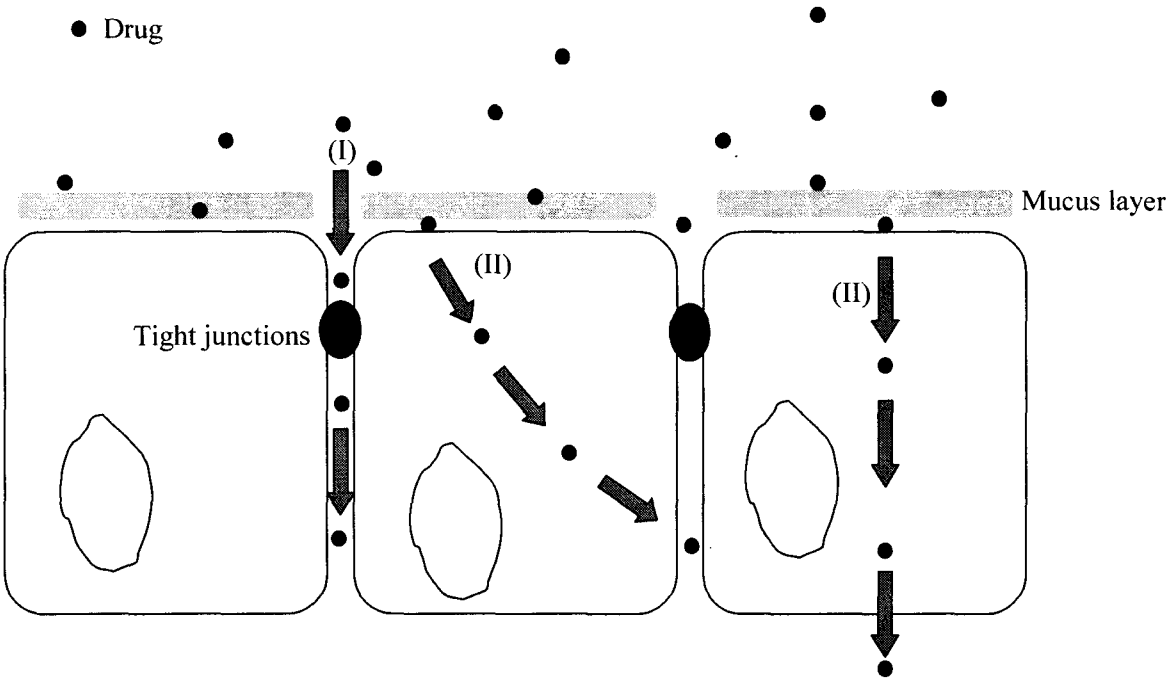

Figure 2. Drug transport pathway across mucosa membrane
(I) paracellular pathway, (II) transcellular pathway

absorption site by the mucociliary clearance mechanism. To improve the low absorption and to control the drug concentration in plasma, two main strategies have been used; modification of permeability across the nasal membrane by the use of absorption enhancers, and a mechanical approach using bioadhesive gel system and various dosage forms.

Budesonide used in *Chapter I* is steroidal drug for asthma, allergic and seasonal rhinitis (*Figure 3*). Considering the effective therapeutic regimens for budesonide, pharmaceutical dosage form of sustained release type will be desired for increase of the bioavailability, keeping the effective therapeutic level for a long time, and avoiding the unexpected side effects. Therefore, I developed pH-sensitive and mucoadhesive polymer system in which the polymer works as membrane-disruptors and adhesive agents at the pH of nasal mucosa (*Figure 3*), and thereby the system can continuously

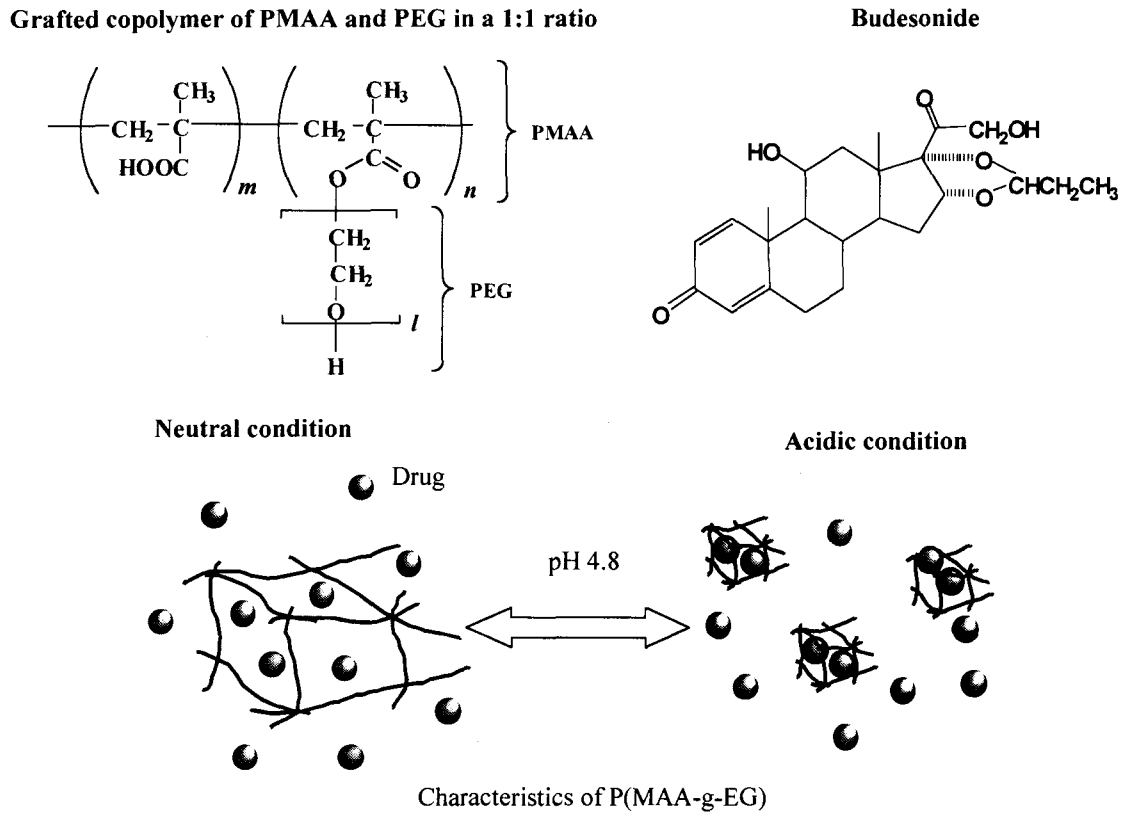

Figure 3. Chemical structures of P(MAA-g-EG) copolymer and budesonide, and characteristics of P(MAA-g-EG)

release the drug from the polymer.

In *Chapter II*, to increase drug absorption, I discussed novel enhancers, β-sitosterol β-D-glucoside (Sit-G), the main component of soybean-derived sterol glucoside (SG) and β-sitosterol (Sit), the main component of soybean-derived sterol (SS). Sit has the similar structure with cholesterol as shown in *Figure 4*, which is mainly contained in plants. In the pharmaceutical field, these compounds were used as the excipients and emulsifiers. Furthermore, it is known that Sit inhibits the uptake of cholesterol showing higher affinity to biological membrane than cholesterol [5,6], and induces the inhibition of proliferation, and apoptosis of tumor cells [7-9]. On the other hand, SG and Sit-G are potential carrier for selective liver targeting due to accumulation into liver [10,11]. Furthermore, Sit-G has the antihyperglycemic effect as the pharmacological

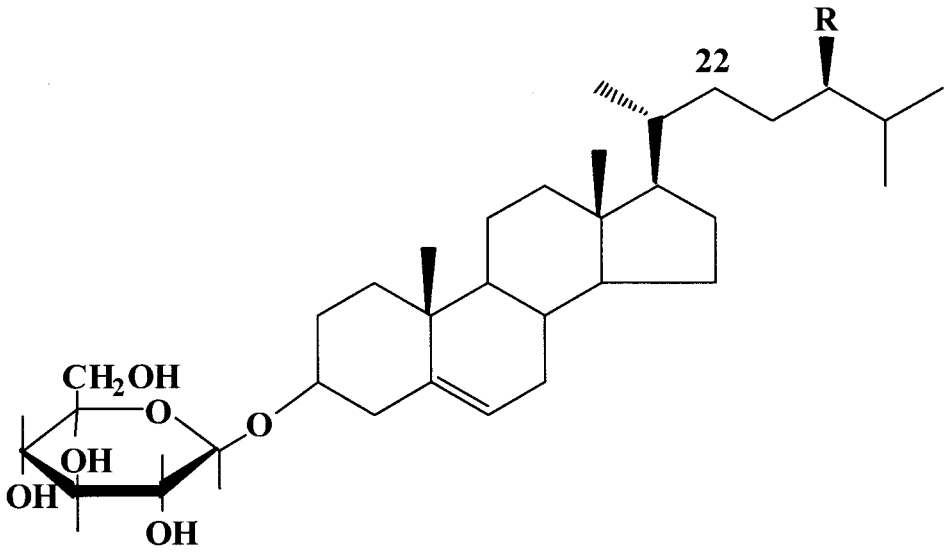

Figure 4. Chemical structure and components of soybean-derived sterylglucoside (SG)
β-Sitosterol β-D-glucoside (Sit-G); R=C_2H_5 (49.9 %)
Campesterol β-D-glucoside; R=CH_3 (29.1 %)
Stigmasterol β-D-glucoside; R=C_2H_5 and Δ^{22} (13.8 %)
Brassicasterol β-D-glucoside; R=CH_3 and Δ^{22} (7.2 %)

effect due to a stimulation of insulin secretion from pancreatic β-cells [12]. Recently, the absorption enhancing effect of Sit-G and Sit for nasal delivery was reported without inducing the irritation to nasal mucosa [13,14]. However, the enhancing effect by the enhancers was attempted to only insulin, and the mechanisms of enhancer action are still unclear. Fully understanding these mechanism is of importance for therapeutic applications.

To increase the bioavailability by the increase of residence time and interaction of the formulation on the nasal mucosae, various dosage forms such as powders, emulsions, liposomes and nanoparticles (NP) have been used. In *Chapter III*, NP based on Sit or Sit-G was developed to improve their low solubility and to avoid incomplete dispersion in water.

In *Chapter I*, the release of the drug from mucoadhesive and pH-sensitive copolymers in nasal delivery was discussed. In *Chapter II*, the enhancing effect by Sit

and Sit-G, and their mechanisms were investigated, focusing on the lipid bilayer barrier, as well as transcellular/paracellular pathways. In *Chapter III*, the enhancing effects of the NP dosage forms based on Sit or Sit-G were discussed for nasal absorption.

Chapter I

Release Profiles of Budesonide from Mucoadhesive, pH-Sensitive Copolymers for Nasal Delivery

1. Introduction

To provide the sustained drug absorption, bioadhesive polymers have been used. Highly swellable, anionic hydrogels that exhibit mucoadhesive behavior could be extremely useful in nasal delivery applications (*Table 1*) [15]. Such gels would swell significantly when in contact with the mucosa (pH of almost 7 in nasal mucus) and release the drug in a continuous fashion while adhering to the mucosa. At this point, a pH-sensitive, hydrogel based poly(methacrylic acid) (PMAA) grafted with poly(ethylene glycol) (PEG) ((P(MAA-g-EG)) was selected. Because of the unique chemical structure, the gel swells in neutral or basic conditions due to the ionization of the pendant acid groups and deswells in acidic media owing to the interpolymer complexation between PEG and PMAA [16] as shown in *Figure 3*. Additionally, the gel strongly adheres to the mucosa when it was in the highly swollen conformation [17].

Table 1. Bioadhesive polymers enhancer used for nasal mucosa

Arginate
Carbopol
Carboxymethylcellulose
Chitosan
Hydroxyethylcellulose (HEC)
Hydroxypropylcellulose (HPC)
Hydroxypropylmethylcellulose (HPMC)
Methylcellulose (MC)
Pulronic F127
Starch
Tamarind gum
Xanthan gum

The drug selected for this study was budesonide. Budesonide is a derivative of 16-α-hydroxypredonisolone, and is reported to have low bioavailability (10.7 %) following oral administration [18]. Nasal administration of budesonide is used for the treatment of allergic and seasonal rhinitis, and is also effective for asthma. Therefore, controlled systemic circulation of the drug is required to improve the therapeutic efficiency.

In *Chapter I*, I investigated the loading of the drug into the polymeric microparticles, the *in vitro* release kinetics and the pharmacokinetics following intranasal administration of the drug-containing gels in rabbits.

2. Experimental Section

2-1. Materials

Budesonide with a mixture of two epimers was purchased from Sigma Chemical Co. (St. Louis, MO). P(MAA-g-EG) microparticles containing a 1:1 molar ratio of PMAA and PEG chains of 1,100 molecular weight were prepared as described previously [17]. The polymers used contained a nominal molecular weight between crosslinking of 6,000. The structures of the budesonide and the copolymers are shown in *Figure 3*. All other reagents were of analytical grade or best.

2-2. Drug loading in polymer and analysis of drug

Budesonide (3 mg) was dissolved in 10 mL ethanol or ethanol solutions of various concentration; 50 % ethanol solutions adjusted with trisaminomethane-HCl buffer (Tris-buffer) to pH 7.19 and 25 % ethanol solutions adjusted with Tris-buffer or NaOH to pH 7.23 and 7.30, respectively. Initially dry copolymer microparticles were dispersed in the drug solutions and stirred at a constant rate for one day. The weight ratio of drug to polymer in the initial solution was varied from 1:1 to 1:3. At specified time points, 100 μL samples were withdrawn from the solutions using filtered syringes (Ishikawa Manufactory Co.). The budesonide concentration in each sample was measured by HPLC. N-propyl-p-hydroxybenzoic acid-methanol solution was used as an intrastandard. The HPLC system (LC-10 AS, Shimadzu Co. Ltd.) was equipped with a UV detector (SPD-10AV, Shimadzu Co. Ltd.) at 254 nm. The mobile phase, consisting of a water/ethanol mixture (57/43 by volume), was eluted through a reverse-phase column (3.9 x 150 mm (*in vitro*) and 4.6 x 150 mm (*in vivo*)) packed with Nova Pak C18 (Waters, Milford, USA) at rate of 0.5 mL/min at room temperature.

Following drug loading, the solutions were filtered using 1 μm filter paper and an equal volume of the first fluid (JP XIII) was added to deswell the drug-loaded particles. These P(MAA-g-EG) hydrogels containing budesonide were dried *in vacuo* for 3 days and stored at 4 °C prior to use in further studies [19].

2-3. Release studies of drug from budesonide-polymer

Budesonide-containing microparticles (3 mg) were dispersed in 30 mL of a 25 % ethanol solution adjusted with NaOH to pH 7.30 and stirred at a constant rate. At regular intervals, 200 μL samples were withdrawn using a filtered syringe. After each sample was removed, an equal volume of the ethanol solution was returned to the solution. Budesonide concentration in each sample was measured by HPLC.

2-4. Preparation of budesonide dosage forms

Budesonide solution for intravenous administration was prepared by dissolving the drug in an ethanol solution and diluting the solution with saline so that the final concentration of ethanol was about 50 %. A mixture of 2:1 (weight) of budesonide:lactose was dissolved in 30 % ethanol solution and freeze-dried. Budesonide-containing copolymers (budesonide:copolymer = 1:1, weight) could be administered alone to achieve the desired dosage because low drug content in polymer and the limited volume of nasal cavity. Therefore, the powder dosage form which consisted of a 1:1 (weight) physical mixture budesonide/lactose and budesonide-containing polymer was used. The samples for nasal administration were passed through a 200-mesh sieve to yield particles with a radius of 75 μm or less and were stored at 4 °C until use.

2-5. Animal experiment

Male Japanese rabbits weighing between 2.5 and 3 kg were obtained from Saitama Experimental Supply (Japan) and used through all experiments. For the animals receiving intravenous budesonide, about 1 mL of budesonide solution containing 2 mg/kg body weight dose was injected in the rabbits. The nasal administration was carried out by the following methods. A polyethylene tube with inner diameter of 0.97 mm, outer diameter of 1.27 mm and length 10 cm (Netsuke Seisakusyo Co. Ltd.) was attached to the top of a syringe and inserted in the nasal cavity about 2.0 cm from nostril. Nasal administration was limited to one side of a nasal cavity in each experiment. Powder dosage form was loaded into the syringe and administered through the tube into the site of the nasal cavity using the procedure previously described [20].

The powder dosage form of budesonide was administered to rabbits at a dose of 2 mg budesonide/kg. After each time point, 200 μL blood samples were collected serially from the ear vein of the animals. The plasma samples were separated by centrifugation at 13,000 rpm for 3 min, and then the protein was extracted by addition of 1 mL isopropanol/dichlromethane to 100 μL plasma samples. The organic acid phase was taken in a test tube and evaporated by gentling heating in a N_2 stream. The residue was dissolved in 200 μL of the mobile phase described above. The samples were injected into HPLC system to determine the budesonide concentration.

The experimental procedures described above were performed according to the rules set by the Committee on Ethics in the Care and Use of Laboratory Animal in Hoshi University.

2-6. Analysis of pharmacokinetic data

The total area under budesonide concentration-curve (AUC) from time 0 to 8 hr was estimated from the sum of successive trapezoids between each data point. Bioavailability (F) was defined on the basis of AUC according to the following equation:

$$F = \frac{AUC_{nasal}/Dose_{nasal}}{AUC_{i.v.}/Dose_{i.v.}} \times 100 \qquad \text{Eq. 1.}$$

where AUC_{nasal} and $AUC_{i.v.}$ represent AUC after nasal administration and intravenous administration of 2 mg budesonide/kg in rabbits, respectively.

The mean residence time (MRT hr) were determined using MULTI [21].

2-7. Data analysis

For group comparison, the one-way layout analysis of variance (ANOVA) with duplication was applied. Significant differences in the mean values were evaluated by Student's unpaired *t*-test. A p value of less than 0.05 was considered significant.

3. Results and Discussion

Budesonide is a poorly soluble drug in water. On the other side, P(MAA-g-EG) swells to a high degree in water when the pH is greater than 4.8 [16]. In order to optimize the loading conditions for budesonide in this polymer, the uptake and release behavior of the drug were examined in ethanol/water solutions of various concentrations at physiological pH.

3-1. Drug loading efficiency and release study

The uptake profile of budesonide into P(MAA-g-EG) in ethanol solutions is shown in *Figure 5* at an initial drug/polymer ratio of 3 in the solution. Less than 10 % of the budesonide were incorporated into the polymer in pure ethanol and 50 % ethanol solution adjusted with Tris-buffer. However, in the solutions with decreased amounts of ethanol, 25 % ethanol solutions adjusted with NaOH and Tris-buffer, nearly 50 % of budesonide partitioned into the polymer (*Figure 5*). The uptake profiles for both solutions were nearly identical.

The difference in the uptake behavior of the polymer in the different solutions can be attributed to the pH-dependent swelling behavior of the P(MAA-g-EG) hydrogels. The polymer networks swell due to electrostatic repulsions between dissociated carboxyl groups of PMAA under neutral or basic conditions in media with high dielectric constants like water [16]. The swelling behavior of these gels is reduced when the degree of ionization of the PMAA is reduced in solutions with low dielectric constants as in the case of solutions containing high concentrations of ethanol [16]. The uptake of drug in the polymers was very low in the 50 % ethanol and pure ethanol

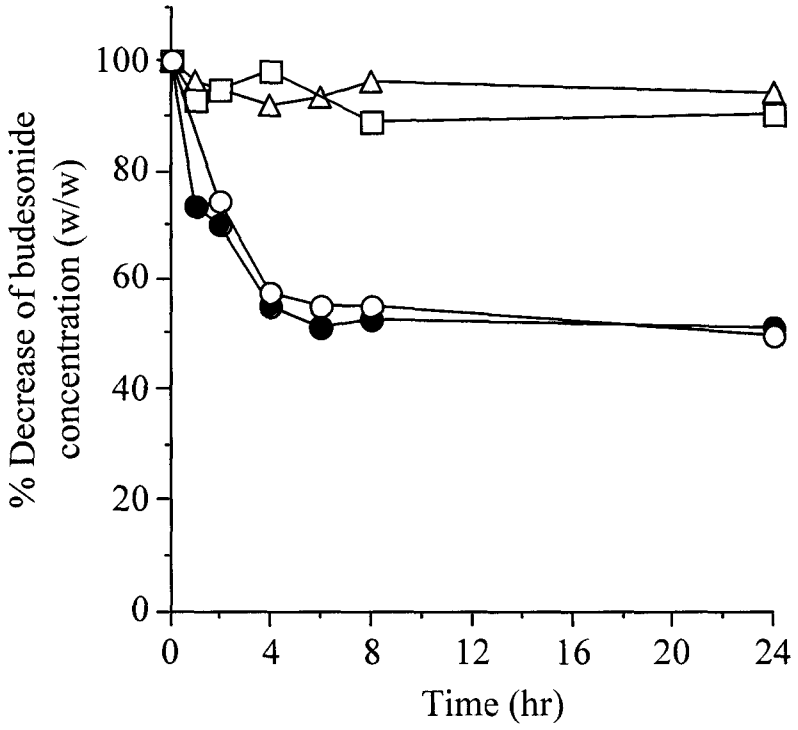

Figure 5. % Decrease of budesonide by uptake to polymer (w/w) in various ethanol aqueous solutions adjusted with NaOH and trisaminomethane-HCl buffer at the 1:3 ratio of drug to polymer at 25 °C
□: ethanol, △: 50 % ethanol aqueous solution adjusted with buffer at pH 7.19, ○: 25 % ethanol aqueous solution adjusted with buffer at pH 7.23, ●: 25 % ethanol aqueous solution with NaOH at pH 7.30)

solutions because the swelling of P(MAA-g-EG) was significantly inhibited and the drug did not partition into the collapsed gel (*Figure 5*). However, in solutions with less ethanol, the gels swelled to a greater degree and the drug was incorporated more favorably into the highly swollen networks. Each of the solutions had pH values very close to 7. Therefore, the uptake of hydrophobic drugs such as budesonide into P(MAA-g-EG) was affected by the organic solvent concentration more than by the solution pH.

The initial budesonide/polymer weight ratio in the solution also had an effect on the degree of loading of budesonide in the polymer. The decrease of solution budesonide concentration is shown in *Figure 6* for different initial drug/polymer weight ratios in

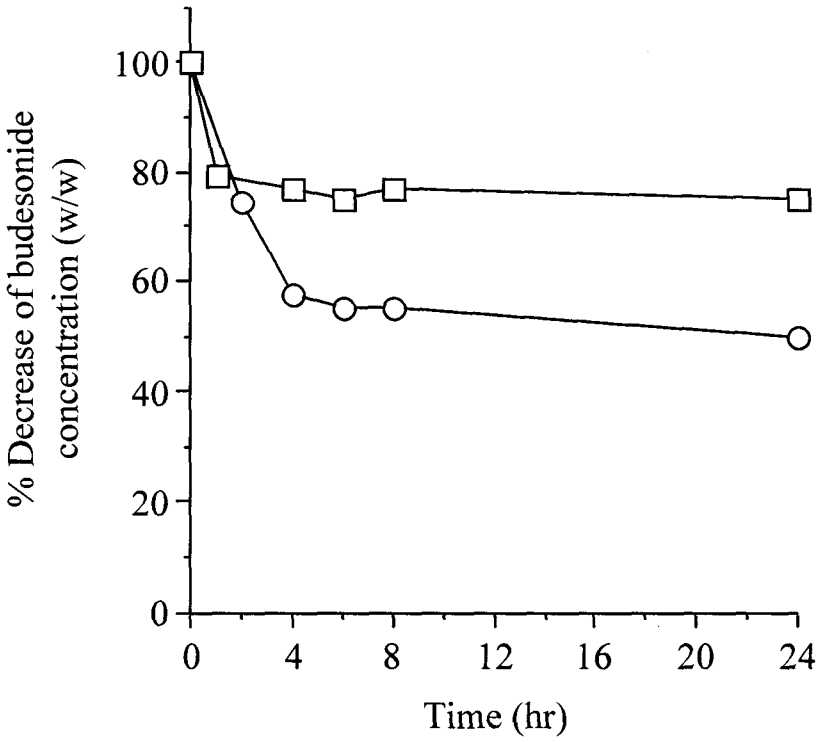

Figure 6. % Decrease profiles of budesonide by uptake to polymer (w/w) at various ratios of drug to polymer in 25% ethanol aqueous solution adjusted with NaOH at pH 7.30 at 25 °C
□: drug : polymer = 1 : 1, ○: drug : polymer = 3 : 1 (w/w)

25 % ethanol adjusted to pH 7.3 using NaOH. The decrease of the budesonide concentration in the drug solution was significantly greater in the solutions containing a larger weight ratio of drug to polymer. In this case, the partitioning of the drug into the polymer increased with increasing drug concentration.

Applying these drug-containing polymers for nasal delivery, it is desirable to have a large concentration of drug within the polymer. Therefore, hydrogels for nasal absorption studies were prepared in 25 % ethanol solutions with pH 7.30 and initial drug:polymer weight ratios of 3. After soaking the swelling copolymers for 24 hr in the drug solutions, the microparticles were dried as described above.

The release behavior of the budesonide-loaded microparticles is shown in *Figure 7*. The release ratio, defined as the ratio of the amount released at any time (M_t) to total

amount released after 8 hr (M_∞), is plotted as a function of time (*Figure 7A*). The release of budesonide from budesonide-polymer showed rapid burst, where about 60 % budesonide were released less than 30 min. For the remainder of the time, the release behavior appeared to be followed by a classical Fickian mechanism. The type of release behavior was evaluated by plotting the release ratio, $\left(M_t/M_\infty\right)$, as a function of the squared root of time (*Figure 7B*). After the initial burst, a linear relationship between the release ratio and $t^{1/2}$ was seen. This type of profile indicates that the release behavior of budesonide from the gel was governed by an initial burst due to rapid gel swelling followed by the diffusion of drug from the gels [22].

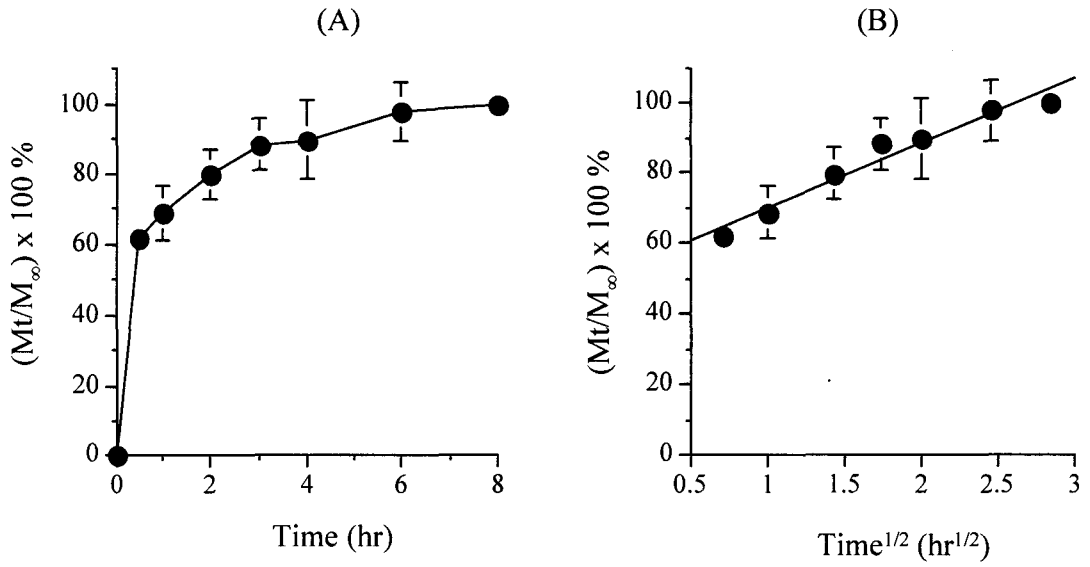

Figure 7. Release profiles of budesonide from polymer microparticles plotted as a function of (A) time and (B) time$^{1/2}$
Each value represents as means ± S.D. (n=3).

3-2. Nasal administration of budesonide/polymer

The plasma budesonide concentration profiles following intravenous and nasal administration of budesonide solution and budesonide/polymer are shown in *Figure 8.*

Following nasal administration of the polymeric formulations, the peak plasma concentration was reached at about 45 min, indicating an initial rapid release of budesonide from the polymer and absorption of budesonide through the nasal mucosa. After the initial burst, the concentration in plasma remained fairly constant for a minimum of 8 hr. This indicates that the budesonide was continuously released from the polymer due to diffusion. In comparison, following intravenous administration of budesonide, the plasma concentration peaked immediately and decreased rapidly over the next 4 hr. At 5 hr following the intravenous administration, the plasma concentration of budesonide had decreased to nearly undetectable levels.

The pharmacokinetic parameters are shown in *Table 2*. The bioavailability of budesonide following nasal administration of the polymeric formulation was 83.9 %. The bioavailability was increased by durability of the drug concentration in plasma despite budesonide has a short elimination half life ($t_{1/2}$=29 min). Following extravascular administration of a drug powder dosage form, the observed total MRT is

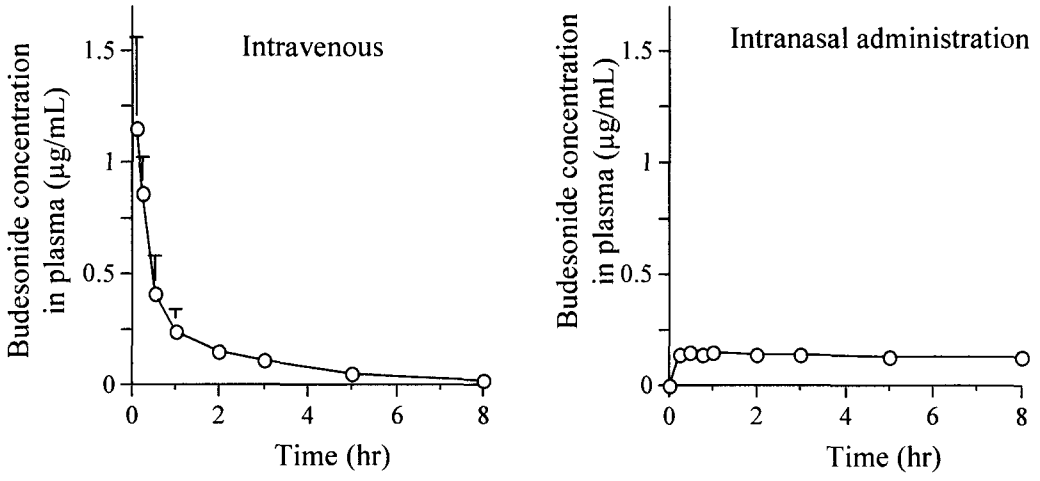

Figure 8. Plasma concentration profiles after intravenous administration of budesonide solution and intranasal administration of budesonide/polymer at a dose of 2 mg/kg budesonide in rabbits
Each value represents as means ± S.D. (n=4).

Table 2. Pharmacokinetic parameters of budesonide following intravenous and nasal administration of budesonide solution and budesonide/polymer, respectively, at a dose of 2 mg/kg budesonide in rabbits

	AUC_{0-8} ($\mu g \cdot hr \cdot mL^{-1}$)	MRT (hr)	VRT (hr^2)	F [a] (%)
Intravenous				
Budesonide solution [b]	1.24	1.69	3.34	100
Intranasal				
Budesonide/polymer [c]	1.04	3.95	6.00	83.9

MRT is the mean residence time, and VRT is variance of residence time.
Each value represents the mean.
$t_{1/2}$= 29 min
a) F from 0 to 8 hr
b) Budesonide was dissolved in 50% ethanol aqueous solution.
c) The ratio of budesonide to polymer is 1:1.

the sum of the MRT in the body, i.e., the mean absorption time, the mean dissolution time and the mean release time. The permeation of budesonide might be enhanced by the adhesion of P(MAA-g-EG) to the mucus since the MRT values after nasal administration of budesonide/polymer increased. The total mean dissolution time and the mean release time can be determined 2.26 hr from the difference between the MRT values, after nasal and *i.v.* bolus dose given on separate occasions (*Table 2*). It was reported that bioavailability of drug with the bioadhesive compound such as chitosan [23], and carbopol, i.e., poly (acrylic acid) [24] was increased by bioadhesive action of polymer to the mucus.

Typically, polymers containing carboxylic-acid groups adhere strongly to mucosa due to hydrogen bond interactions in environments where the pH is less than 5, where the carboxylic acid does not dissociate. In this case, the carboxylic acid groups were ionized at pH of approximately 7, however, the strong mucoadhesive characteristics were observed due to the interpenetration of the mobile PEG-grafts and PMAA dangling chains. At this pH, P(MAA-g-EG) hydrogels are highly swollen and the chains are relatively mobile. The mobile chains are able to penetrate the mucosa and

may be able to diffuse into the gels. This chain interpenetration serves as a physical attachment between the gels and the mucosa [17]. In terms of the release characteristics and *in vivo* performance, the drug-containing polymer swelled rapidly within 30 min and released the drug continuously for at least 8 hr. During this period, the hydrogels adhered strongly to the nasal mucosa allowing for the high bioavailability of the drug.

4. Conclusions

The conditions of budesonide loading in a pH-sensitive and mucoadhesive polymer, P(MAA-g-EG), were examined using various ethanol solutions. Ethanol was required for drug solubilization but hindered hydrogel swelling in 50 % ethanol solutions at even pH 7.2. The maximum loading efficiency of the drug in the polymer was obtained using 25 % ethanol solutions at pH 7.3. The release from the drug loaded-polymers was followed by a classical Fickian kinetics after the initial burst. This system was evaluated using nasal absorption in rabbits to confirm whether these gels could effectively deliver the drug in a similar fashion under physiological conditions, such as nasal mucosa. Modulation of the gel swelling and mucoadhesiveness may prove to be useful in the controlled release of drug from pH-sensitive and adhesive polymer at the surface of the nasal mucosa *in vivo*.

Chapter II

Enhancing Effect of β-Sitosterol β-D-Glucoside and β-Sitosterol on Intranasal Absorption of Verapamil and FITC-Dextran 4,400 at Powder Dosage Form

1. Introduction

To increase bioavailability of drug absorption, absorption enhancers such as bile salt [25], cyclodextrin [26] and saponin are co-administered [27]. However, most of them are harmful to nasal epithelium and interfere with nasal mucociliary movement [28,29]. The clinical use of absorption enhancers is not available in Japan except for sodium caprate. Therefore, the search for safe and effective absorption enhancers is an important issue in the both of academia and industry.

Recently, it was reported that SG and SS promoted insulin absorption through nasal mucosae following intranasal administration of suspensions [13] and powder dosage forms with SG [14]. No damages to nasal mucosa were evoked in successive intranasal administration of SG for 5 days [14]. However, the enhancing mechanisms of these compounds have not been clarified yet.

In *Chapter II*, I examined the activity of these enhancers on nasal absorption of verapamil and FITC-dextran 4,400 (FD-4) as model drugs, employing powder dosage forms in rabbits. Intranasal administration of verapamil seems to be the suitable since

Table 3. Bioavailability of verapamil and FD-4 through the various administered sites

Drug	Animal	Administrered route	Dose (mg/kg)	Formulation	Enahncer	F (%)	Ref.
Verapamil	Dog	Oral	2.5	Solution	-	13 ± 3	[30]
		Nasal	0.75		-	36 ± 7	
FD-4	Rat	Nasal	10	Solution	-	2.2 ± 1.3	[4]
					1 % w/v Glycocholate	11.7 ± 2.0	
					1 % w/v Taurocholate	11.5 ± 2.0	
					1 % w/v EDTA	10.1 ± 1.9	
					1 % w/v C10	13.0 ± 3.0	
		Pulmonary	5	Solution	-	7.2 ± 1.1	[31]
					1 % w/v Glycocholate	29.0 ± 1.5	
					1 % w/v EDTA	19.4 ± 2.4	
					1 % w/v C10	31.8 ± 2.3	
	Rabbit	Nasal	1	Microsphere (powder)	Lactose	9.1 ± 3.8	[32]
					Chitosan	12.6 ± 4.5	
					Carbopol 934P	32.7 ± 13.2	
	Pig	Buccal	0.22	Solution	-	1.8 ± 0.5	[33]
					10 mM Sodium glycodeoxycholate	12.7 ± 2.8	

this drug was subject to the extensive first-pass metabolism in the liver when administered orally [30] (*Table 3*). Further enhancement of bioavailability of verapamil will be attained by the use of enhancer. FD-4 is not therapeutic drug, but is extensively used for evaluating the enhancer's activity because of its poor absorption in various sites (*Table* 3).

The second aim in this chapter is to elucidate the mode of action of SG and Sit-G. Absorption enhancers are classified into two groups. The first one is the paracellular type such as calcium chelator [31] and some compounds by which intracellular calcium levels were increased [32,33]. Another one is transcellular type such as acylcarnitines (*Table 4*) [37]. Sodium caprate (C10) such as typical enhancer of paracellular type induced the opening of tight junctions, which brought about the decrease of transepithelial resistance (TEER) accompanied with increase of intracellular calcium levels ($[Ca^{2+}]i$) [32,33]. On the other hand, enhancement mechanism of transcellular type is attributed to the perturbation of the lipid bilayer. Change of $[Ca^{2+}]i$ and TEER values were monitored to estimate contribution of paracellular pathway. At the same time, the calcein leakage from liposomes as a model biomembrane was determined to evaluate the role of transcellular pathway.

Table 4. Classes of absorption enhancers

Enhancing route	Absorption enhancers
Parapacellular route	Chitosan
	EDTA
	Didecanoylphosphatidylcholine
	Glycyrrhetic acid derivative
	Unsatrurated fattty acid (C10)
	NO donor
Transcellular route	Acylcarnitine
	Bile salt (sodium glycocholate, sodium deoxycholate)
	Methylated b-cyclodextrin
	Saponin
	Saturated fatty acid (Oleic acid)

2. Experimental Section

2-1. Materials

SG (M.W. 573.32) and SS (M.W. 409.17) were kindly supplied by Ryukakusan Co. Ltd., (Tokyo, Japan). Sit was purchased from Tama Biochemical Co. Ltd. (Tokyo, Japan). Sit-G (M.W. 578.84) was purchased from Essential Sterolin Products Ltd. (Midrand, South Africa), and the purity of Sit-G was identified and determined to be more than 96 % by ^{13}C-NMR and thin layer chromatography (data not shown). Verapamil hydrochloride, FD-4, cremophor EL, dimethyl sulphoxide (DMSO), and dulbecco's phosphate-buffered saline (D-PBS) were purchased from Sigma Chemical (St. Louis, MO). Oleic acid (M.W. 282.5), C10 and calcein were purchased from Tokyo Kasei Kogyo (Tokyo, Japan). Fura PE3-AM was purchased from Wako Pure Chemical Industries, Ltd. (Osaka, Japan). Egg phosphatidylcholine and cholesterol were purchased from NOF Corp. (Tokyo, Japan). All other chemicals were obtained from commercial sources and were of analytical reagent grade.

2-2. Preparation and administration of dosage form

The intranasal administration was described in *Chapter I.* The FD-4 and verapamil powder dosage forms were prepared by freeze-drying of the following solution (verapamil: 75 mg verapamil, 225 mg lactose as control, SG, and Sit-G, FD-4; 100 mg FD-4, 200 mg lactose, Sit-G and Sit), and sieved through 200-mesh (particle size less than 75 μm). The physical form of verapamil hydrochloride in all powder formulations measured by X-ray diffraction apparatus (RINT 1400, Rigaku, Co. Tokyo) was amorphous (data not shown). The 3 mg/kg of each powder dosage form of verapamil and FD-4 was administered intranasally to Japanese male rabbits weighing

2.5 – 3.0 kg at 0.75 mg verapamil/kg, and 1 mg FD-4/kg by the previously reported method [14]. The liquid dosage forms consist of two types such as suspension and solution. The former was prepared by the sonication of 1 % w/v Sit or Sit-G sieved through 200 mesh (75 μm) in saline since Sit and Sit-G are far solubility in water. The latter was 1 % w/v C10 in saline. Aliquots of 200 μL each liquid dosage form were administered via one nostril of rabbits [38].

For intravenous administration, verapamil hydrochloride and FD-4 (75 mg/mL and 15 mg/mL in saline, respectively) was injected into the ear vein of rabbits at a dose of 0.75 mg verapamil/kg, and 1 mg FD-4/kg, respectively.

2-3. Determination of verapamil and FD-4

At each time point, blood sample was taken from ear vein, and then performed the centrifugation at 13,000 rpm for 3 min to obtain plasma.

For the determination of verapamil in plasma, to 100 μL plasma samples, 1 mL acetonitorile containing 140 ng/mL butyl *p*-aminobenzoate was added as an internal standard. Samples were mixed with a vortex mixer and centrifuged at 13,000 rpm for 5 min. The organic solvent was evaporated at 50 °C under a gentle stream of nitrogen and the residues were dissolved in 200 μL of HPLC mobile phase. A 50 μL of this solution was injected into an HPLC equipped with a fluorescent detector. The instruments consisted of a Shimadzu LC 10AL liquid chromatography, SIL 10 A autoinjector, CR-6A chromatopac, SCL 10A system controller and RF-10ALXL fluorescent detector (Shimadzu, Kyoto). The detector setting was 275 nm for excitation and 315 nm for emission [39]. A 3.9 x 300 mm column packed with Nova Pak C18 (Waters, Milford, USA) was employed. The mobile phase was

acetonitorile:0.13 M KH_2PO_4 solution (40:60) pumped at a rate of 1.0 mL/min [39].

For the determination of FD-4 in plasma, 100 μL plasma samples were added in 900 μL PBS and FD-4 concentration was measured by fluorescent spectrometer (Hitachi F-4010, Tokyo) at an excitation wavelength of 490 nm and emission wavelength of 520 nm.

2-4. Analysis of pharmacokinetic data

The AUC values of verapamil and FD-4 from time 0 to infinity for verapamil, and 3 hr for FD-4were estimated from the sum successive trapezoids between each data point, respectively. Bioavailability (F) was calculated according to Eq. 1 in *Chapter I* after intravenous administration of 0.75 mg verapamil/kg, and 1.0 mg FD-4/kg in rabbits, respectively.

The maximum concentration (Cmax), the time reached at Cmax (Tmax), and MRT were determined using MULTI [21].

2-5. Measurement of FD-4 and enhancers following administration of powder dosage form in vitro

After rabbits were sacrificed by injection of 85 mg/kg pentobarbital solution into the ear vein, the nasal septum was removed and the excised nasal mucosa was mounted in Franz-type diffusion cell with an available diffusion area of 1 cm^2. The receiver side was filled with 16 mL Ringer's solution containing 125 mM NaCl, 5 mM KCl, 1.4 mM $CaCl_2$, 1.2 mM KH_2PO_4, and 11.0 mM D-glucose (pH 7.4) saturated with 95 % O_2-5 % CO_2 gas at 37 °C. Two mg of FD-4 powder dosage form with enhancers (FD-4:enhancer = 1:2 weight) was applied to the nasal mucosa using the same device as

in vivo study, and 1 mL sample was taken from the receiver side to measure the amount of permeated FD-4 after 30 min. To remove the excess powder from the nasal mucosae, the mucosae after permeation study were washed with Ringer solution for three times, and then the following procedures. To estimate FD-4 uptake into the nasal mucosa, after extraction of lipids the mucosa was homogenized in 3 mL PBS, and FD-4 concentration in the sample was measured as described above. To estimate the uptake of enhancers and the remaining amount of cholesterol at the surface and in the nasal mucosa, the mucosa was washed with ethanol, and extracted using a 2:1 v/v mixture of methanol and chloroform. Cholesterol, Sit and Sit-G were analyzed by HPLC. A 3.9 x 150 mm column packed with Nova Pak C18 (Waters, Milford, USA) was employed. The mobile phase was methanol pumped at a flow rate of 0.5 mL/min.

2-6. Induction of calcein leakage from liposomes by enhancer

Liposomes entrapped with calcein were prepared with 70 μmol egg phosphatidylcholine and 30 μmol cholesterol according to the reverse-phase evaporation method [40,41]. A liposome-1/10 diluted PBS (1/10 PBS) suspensions was added to methanol-1/10 PBS in which the enhancer was dissolved and was incubated at 37 °C for 60 min. The calcein leakage was assessed by fluorescence spectrometry with excitation at 490 nm and emission at 520 nm [41]. Calcein leakage was determined from the following equation:

$$\text{Calcein leakage}\,(\%) = \frac{Ft - F_0}{2F_\infty - F_0} \times 100 \qquad \text{Eq. 2.}$$

where F_0 and Ft are the fluorescence intensities of the calcein before and at time t after incubation, respectively, and F_∞ represents the florescence intensity when 100 μL of 10 % Triton X-100 was added to 100 μL sample to completely collapse liposomes with

encapsulating calcein.

2-7. Measurement of $[Ca^{2+}]i$

Fura PE3-AM was loaded into nasal mucosa excised from nasal turbinate of rabbit [42]. Briefly, fura PE3-AM was dissolved in DMSO and mixed with cremophor EL. Nasal mucosa was exposed to 1 μM fura PE3-AM in the presence of 0.04 % cremophor EL in the dark for 5 hr at room temperature. The tissue was rinsed with D-PBS with or without 1.4 mM Ca^{2+} and placed in a bath containing 8 mL D-PBS with or without Ca^{2+} at 37 °C. The tissue was held vertically and equilibrated for 30 min. Then, DMSO was added to a final concentration of about 1 % v/v. After 10 min, 2 mL of 1 % DMSO containing Sit-G (200 μM) was added to the bath followed by 50 μL $CaCl_2$ solution (200 mM) in saline, and finally 4 mL ionomycin solution (26 μM) was added at each time to check fura PE3 adsorption, but inside the cells. $[Ca^{2+}]i$ was measured as the change in fluorescence intensity of fura PE3 bound to calcium with a dual-wavelength fluorometric calcium analyzer, CAF 110 (Japan Spectroscopic, Tokyo, Japan) at 340 nm and 380 nm for excitation and at 500 nm for emission [42].

2-8. Measurement of TEER and FD-4 permeability

The excised nasal mucosa was mounted onto a tissue adapter in Ussing chamber (CEZ-9100, Nihon Kohden, Tokyo). Each chamber was filled with the 10 mL of Ringer's solution. Temperature was kept constant at 37 °C by means of water jackets around the upper reservoirs. The apparent permeability coefficients (*Papp* expressed as cm/sec) were calculated by the following equation;

$$Papp = (dQ/dt)/(C_0 \times A) \qquad \text{Eq. 3}$$

where dQ/dt is the flux, C_0 is the initial concentration of FD-4 on the mucosal side and A is the surface area (0.673 cm^2).

For measurement of short-circuit current (Isc μA), the potential differences (PD) were maintained at 0 mV with an automatic voltage clamp system. Isc and PD were monitored at 10 min intervals for up to 120 min. TEER was calculated following Ohm's low, $\text{TEER}\,(\Omega) = \frac{\text{PD}\,(\text{mV})}{\text{Isc}\,(\mu\text{A})} \times 1000$. TEER values are given as percentages of the baseline TEER recorded prior to the addition of enhancers. The AUC_{TEER} was the calculated area under the TEER change curve from 0 to 120 min.

One mL of 10 % w/v C10, and Sit and Sit-G suspensions were added to the mucosal side to give 1 % w/v as the final concentration of enhancer. One mL samples were taken at 10 min intervals for up to 120 min from the serosal side, and replaced with an equal volume of fresh Ringer's solution. FD-4 concentration was determined by the above method.

2-9. Confocal laser scanning microscopic visualization of FD-4 transport

After the permeation study, the nasal mucosa was fixed with Mildform® 20N at room temperature, and observed by confocal laser scanning microscopy (Radiance 2000, Bio Rad Laboratories, Richmond, CA) linked to a Diaphot® inverted microscope (Nikon, Tokyo, Japan). Vertical and horizontal section images were taken with PlanAPO 60, 1.40 oil objective (Nikon), and FD-4 was excited at a wavelength of 488 nm.

2-10. Data analysis

The data analysis was carried out by the method mentioned in *Chapter I.*

3. Results and Discussion

3-1. Effects of enhancers on intranasal absorption of verapamil and FD-4

SG and SS are very low solubility in water (about 53 μg/mL) and they are used as suspensions, or powder formulation for enhancer and excipient [14,38]. *Figure 9* shows the plasma concentration profile of verapamil after intranasal administration of verapamil powder dosage form with lactose, SG or Sit-G at a dose of 0.75 mg verapamil/kg in rabbits. Cmax of verapamil was reached within 7 min after intranasal administration of each powder dosage form in rabbits. But, Cmax and F value after intranasal administration of verapamil powder dosage form with SG significantly increased compared with those with lactose as control. Moreover, Sit-G, the main

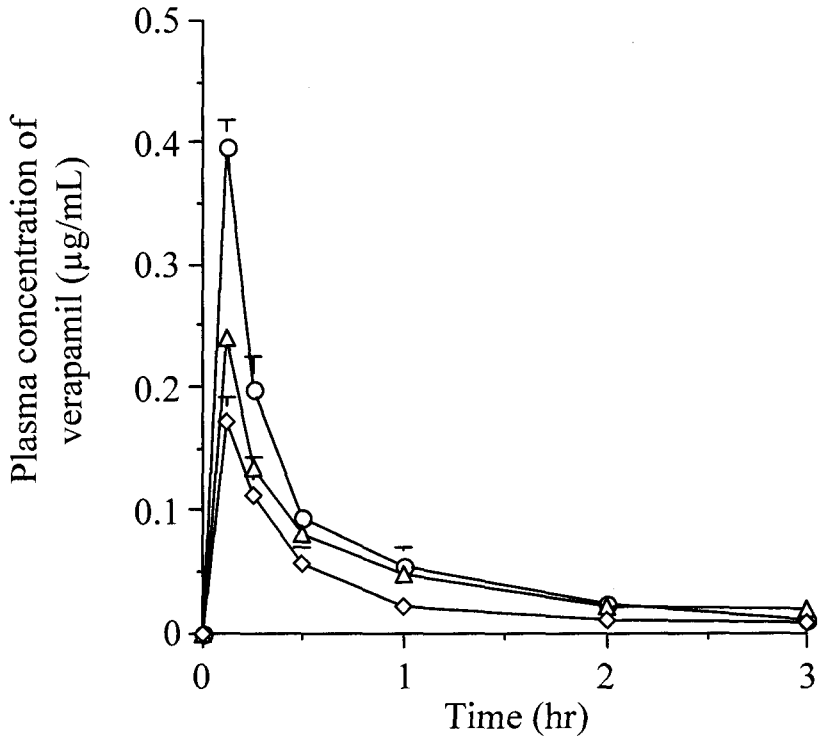

Figure 9. Plasma concentration of verapamil following nasal administration of verapamil powder with or without enhancers in rabbits at a dose of 0.75 mg/kg
◇: lactose, □: SG, ○: Sit-G
Each value represents the mean ± S.E. (n=5).

Table 5. Pharmacokinetic parameters of verapamil following intravenous and intranasal administration of powder dosage forms with enhancers at a dose of 0.75 mg verapamil/kg in rabbits

	Cmax (μg/mL)		MRT [a] (hr)	F [b] (%)	
Intravenous					
Solution	-		1.02 ± 0.12	100	
Nasal					
Powder dosage form [c]					
Lactose	0.171 ± 0.013	**	0.89 ± 0.08	39.8 ± 3.4	**
SG	0.240 ± 0.013	***	1.00 ± 0.06	60.4 ± 3.5	* ***
Sit-G	0.396 ± 0.023	***	0.95 ± 0.13	90.7 ± 9.8	

Each value represents the mean ± S.E. (n=5). * $p < 0.05$, ** $p < 0.01$, *** $p < 0.001$

[a] MRT is the mean residence time, that is the average time of a molecule residues in the body.

[b] F (Bioavailability from 0 to infinity, %) = $AUC_{nasal}/AUC_{i.v.}$ x 100

[c] Drug : enhancer = 1:3 weight

component of SG, increased Cmax and F values up to 1.5 fold compared with that of SG (*Table 5*). However, MRT values following intranasal administration with SG and Sit-G were almost same as that following i.v. though bioadhesive polymer such as chitosan prolonged MRT, which facilitated the drug absorption through mucosa [43]. This result suggests that SG and Sit-G induce significantly faster absorption of verapamil from powder dosage form as i.v. injection.

The influence of Sit and Sit-G on intranasal absorption of FD-4 was investigated by the same method with verapamil. *Figure 10* shows the plasma concentration profile of FD-4 following intranasal administration of powder (A) and liquid (B) dosage forms at a dose of 1 mg FD-4/kg in rabbits. The pharmacokinetic parameters are listed in *Table 6*. Sit-G in the powder dosage form significantly facilitated the nasal absorption of FD-4, i.e., Cmax, AUC, and F values compared with lactose. Tmax for powder dosage forms was 42.5 min for lactose, 16.6 min for Sit and 24.1 for Sit-G, respectively. The plasma concentration profiles for liquid dosage forms were different from those for powder dosage forms. The AUC and F values in liquid dosage forms with Sit and Sit-G were lower than those in powder dosage forms, consistent with the results for

insulin [14,38], although C10, which is used as an enhancer in nasal [42], colonic [44], and rectal mucosa [45], showed the highest Cmax and F values in liquid dosage forms. This difference in the enhancing effect between liquid and powder dosage form suggested that the amount of enhancer in the liquid dosage form contacted with nasal mucosa might be less compared with that in powder one because of their low solubility.

In previous reports, SG and Sit-G facilitated the insulin absorption through the nasal

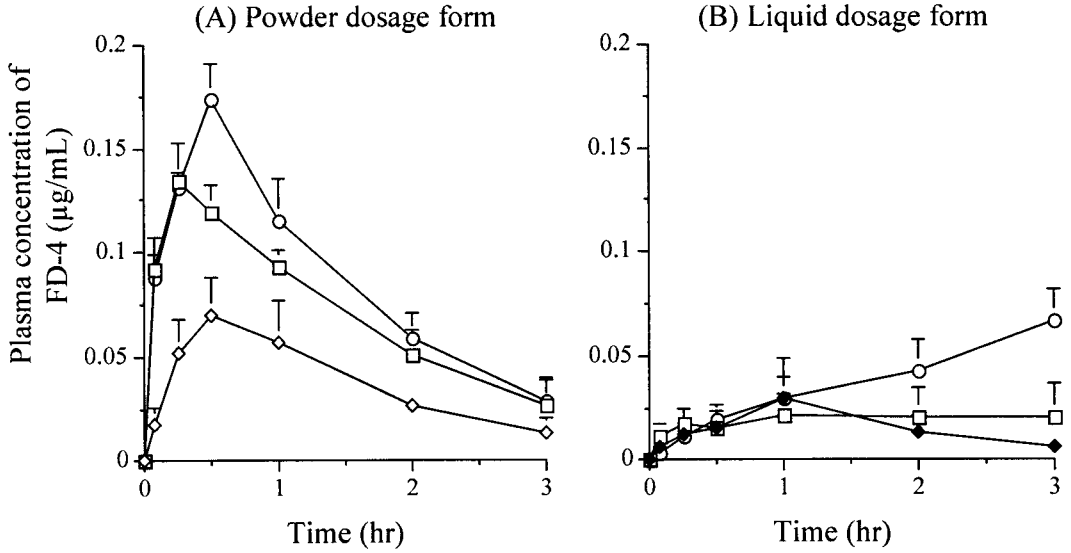

Figure 10. Plasma concentration profile of FD-4 following intranasal administration of powder (A) and liquid dosage (B) forms without or with enhancers in rabbits at a dose of 1 mg FD-4/kg
◇: lactose, ◆: PBS, □: Sit, ○: Sit-G
Each value represents the mean ± S.E. (n=4-6).

Table 6. Pharmacokinetic parameters of FD-4 following intranasal administration of liquid and powder dosage forms with enhancers at a dose of 1 mg FD-4/kg in rabbits

	Cmax (μg/mL)	Tmax (min)	MRT [a] (hr)	F [b] (%)
Powder dosage form				
Lactose	0.070 ± 0.019	42.5 ± 19.0	64.0 ± 8.4	4.1 ± 1.1
Sit	0.134 ± 0.019	16.6 ± 3.5	63.8 ± 7.5	6.9 ± 0.4
Sit-G	0.174 ± 0.017	24.1 ± 2.5	63.8 ± 4.6	8.3 ± 1.0
Liquid dosage form				
Saline (control)	0.013 ± 0.012	-	69.1 ± 18.0	1.4 ± 0.3
1 % w/v C10	0.320 ± 0.100	-	26.6 ± 12.8	8.2 ± 2.9
1 % w/v Sit suspensions	-	-	70.6 ± 8.8	1.8 ± 1.1
1 % w/v Sit-G suspensions	-	-	103.6 ± 16.9	3.0 ± 0.9

Each value represents the mean ± S.E. (n=5). * $p < 0.05$, ** $p < 0.01$
[a] MRT is the mean residence time, that is the average time of a molecule residues in the body.
[b] F (Bioavailability, %) = $AUC_{nasal}/AUC_{i.v.}$ x 100

mucosa from insulin powder [14], and suspension dosage form [38]. In rabbits, the intranasal administration of insulin powder formulation with 1 % SG resulted in 26.3 % of F value and such powder formulations are superior in providing improved enhancement of insulin transport across the nasal mucosa compared to their suspensions [14,38]. Therefore, it shows that SG and Sit-G facilitate not only insulin but also verapamil and FD-4 absorption through nasal mucosa, indicating they act without special interaction via an insulin exclusive absorption pathway. Furthermore, the efficiency of Sit-G as an enhancer was significantly higher than SG ($p < 0.05$), which agrees with the previous results for insulin (*Table 5*).

For the absorption enhancing mechanism of SG, Ando et al. [38] reported that SG might affect the lipids in mucosal membrane since SG significantly increased the insulin permeation through the artificial lipid membrane consisted of the mixture of n-caprylic acid and lauryl alcohol (4:0.92) compared with SS. However, the detailed enhancement mechanism is unclear. Therefore, I investigated the influence of enhancers on paracellular and transcellular pathway.

3-2. Uptake of FD-4 and enhancers after application of FD-4 powder

Since Tmax values were near 30 min after intranasal administration, the effects of enhancers on the permeated (A) and uptake amounts of FD-4 (B) were examined in the excised nasal mucosa 30 min after application of FD-4 powder (*Figure 11*). The amount of FD-4 permeated through the nasal mucosa was significantly increased by Sit-G and Sit compared with control (*Figure 11A*). Uptake amount of FD-4 with Sit-G significantly increased compared with control and Sit, although the permeated amount of FD-4 with Sit-G was almost the same as that with Sit (*Figure 11B*). The uptake

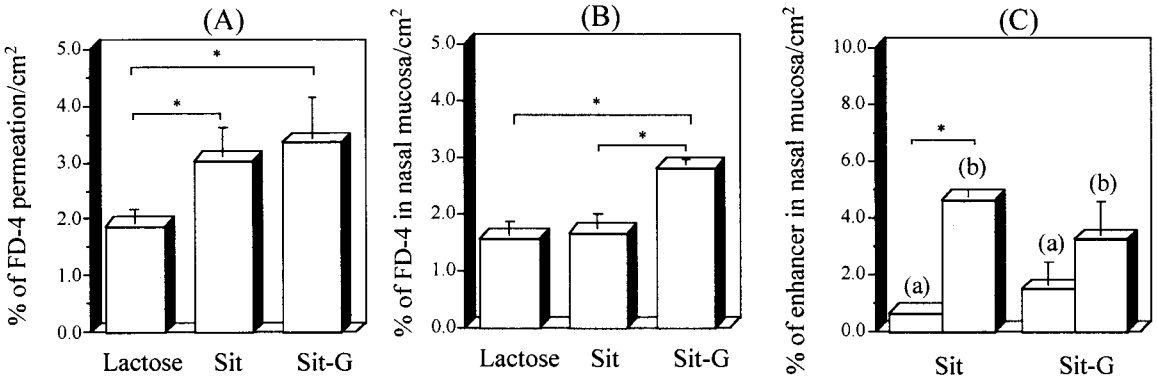

Figure 11. The permeated (A) and remaining (B) FD-4, and uptake of enhancer (C) in 1 cm^2 excised nasal mucosa 30 min after application of 2 mg FD-4 powder dosage forms with enhancers (FD-4:enhancer = 1:2 weight) in Frantz diffusion cells
(a) and (b) in C represent the amount of enhancer in ethanol after washing the mucosal surface, and that in nasal mucosa after extraction with methanol/chloroform (1/2, v/v), respectively
Each value represents the mean ± S.E. (n=4). * $p < 0.05$, ** $p < 0.01$

amount of enhancers and the amount of cholesterol remaining in the nasal mucosa after application of each powder dosage form were measured. Sit amount in the nasal mucosa was significantly higher than that on the surface, but Sit-G showed a greater distribution on the nasal mucosal surface than Sit (*Figure 11C*). These differences may be attributable to the hydrophobicity of the enhancers; Sit is more hydrophobic than Sit-G. Also, the amount of remaining cholesterol was not significantly different compared with control (*data not shown*). These findings were in a good agreement with the observations that Sit-G did not cause the severe damage to nasal mucosa following intranasal administration.

3-3. Calcein leakage from liposomes by enhancers

To investigate the alteration of biological membranes by enhancers using liposomal membrane as a model of biomembrane, calcein leakage from liposomes encapsulating calcein was measured by the incubation with enhancer. Liposomes are often used for biomembrane model [46]. The effect of enhancer to mucosal membrane can be

explained by the measurement and comparison of calcein leakage from liposomes.

Calcein leakage from liposomes by the incubation with SG or Sit-G increased dependently on the enhancer concentration and the incubated time, and these values in SG and Sit-G at 0.5 mM, significantly increased up to 13.2 % and 19.0 %, compared with SS (10.2 %) and Sit (6.6 %) for 60 min at 37 °C, respectively (*Figure 12* and *Table 7*). On the other hand, calcein leakage in SS and Sit was saturated at above 0.2 mM, and appeared to stabilize the liposomes above 16 mol % (0.2 mM) within 30 min (*Figure 12* and *Table 7*).

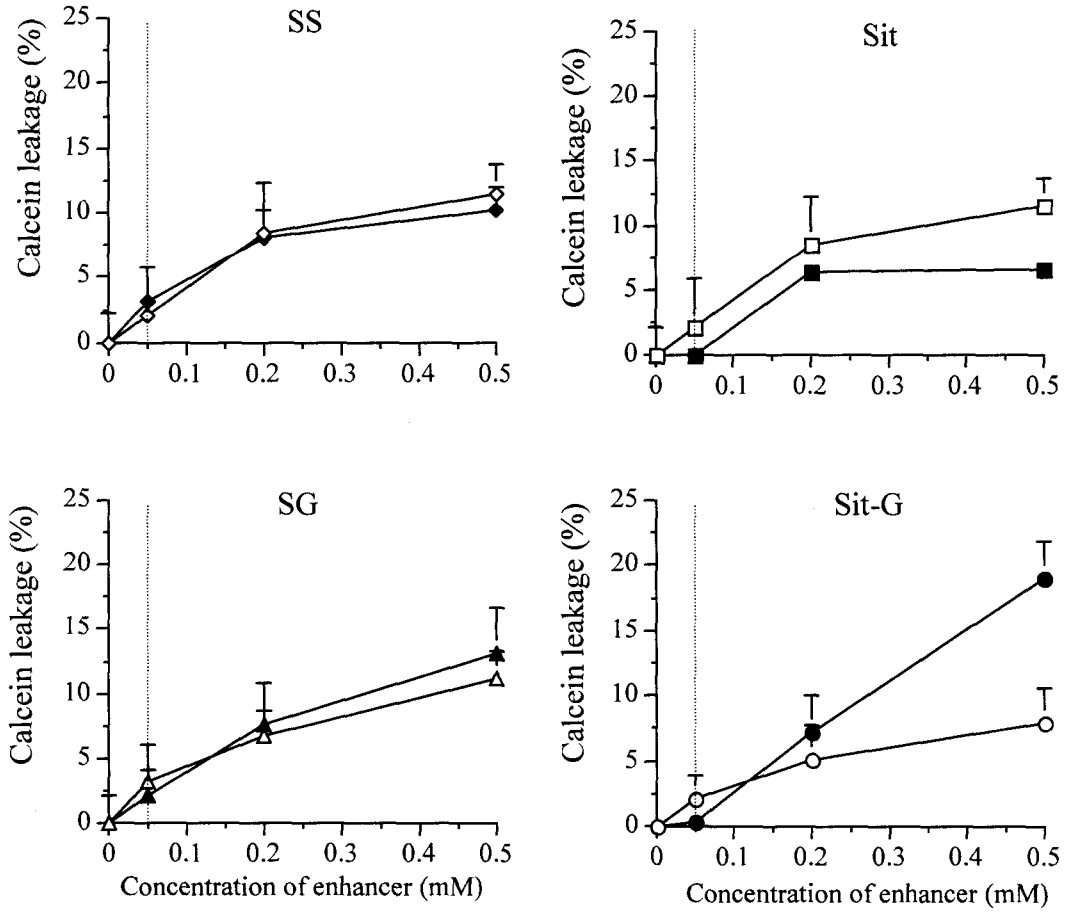

Figure 12. Effect of enhancers on calcein leakage from liposomes with entrapped calcein in methanol-1/10 PBS (1:1) after incubation at 37 °C for 30 min (open symbol) or 60 min (closed symbol)
Total lipid concentration was 1.238 μmol/mL.
Hatched line indicates the solubility of each enhancer in methanol-1/10 PBS (1:1).
Each value represents the mean ± S.D. (n=6).

Table 7. The effect of various enhancers on calcein leakage from liposomes with entrapped calcein after incubation at 37 °C for 60 min

Enhancer (mM)	Calcein leakage (%)		
	0.05	0.2	0.5
Oleic acid	0	0	5.7 ± 3.4
SS	3.1 ± 2.7	8.0 ± 2.2	10.2 ± 1.7
Sit	0	6.5 ± 0.2	6.6 ± 0.9
SG	2.1 ± 2.1	7.6 ± 3.3	13.2 ± 3.5
Sit-G	0.4 ± 0.4	7.2 ± 2.8	19.0 ± 2.9

Each value represents the mean ± S.D. (n=3-6). ** $p < 0.01$, *** $p < 0.001$.
Lipid concentration in methanol and PBS (1:1) was 1.238 μmol/mL.
SG, Sit-G, SS, and Sit were solubilized in methanol-1/10 PBS (1:1), and oleic acid was solubilized in methanol-1/10 PBS (1:1).

Incorporation of Sit into liposomes results in close packing in phospholipid layer compared with cholesterol [47], since Sit increases the order parameter of liposomes calculated from fluorescent anisotropy data at 37 °C [48]. This phenomenon was consistent with *in vivo* data that Sit decreases the membrane fluidity of cells in keratinocytes at 37 °C. Based on these findings, the absorption enhancement by Sit may not be dependent on transcellular pathway since the incorporated Sit made the liposomal membrane rigid.

In contrast, Sit-G may have opposite effect to that of Sit. As described above, SG promoted the insulin permeation through an artificial membrane modified with lipid but Sit did not [38]. Moreover, Muramatsu et al. [47], and Qi et al. [41], reported that the destabilizing effect of SS or SG on liposomes was greater in the order of SS < cholesterol < SG, because SS was closely packed in phospholipid layer, but the glucose group of SG disturbs the optimal packing state. The difference in enhancing efficiency for SG and Sit-G may be due to the characteristic of the sterol side-chain and its role in determining sterol-sterol and sterol-phospholipid interactions as in analogues of cholesterol having different side-chain structure [48,49]. These findings suggested that

SG might promote the drug absorption through transcellular pathway via perturbation of mucosal membrane by SG and Sit-G.

Oleic acid has been used extensively as an enhancer in drug delivery from rectal [50] and buccal [51] mucosa, and has been shown to alter membrane permeability by increasing the motional freedom or fluidity of the membrane phospholipids [52]. Calcein leakage induced by oleic acid increased in a concentration-dependent manner between 0.2 mM and 1.0 mM of oleic acid (*Figure 13A*). Wang et al. [52] reported that oleic acid at 0.1 mM is capable of nonspecific disruption of the alveolar membrane. However, our data suggested that oleic acid might cause little or no disruption but does increase the fluidity of the liposomal membrane, since it resulted in below 40 % calcein leakage.

As shown in *Figure 13B* and *Table 7*, calcein leakage induced by enhancers significantly increased compared with control, and leakage at 0.5 mM enhancers is as following: oleic acid (5.7 %) < Sit (6.6 %) < SS (10.2 %) < SG (13.2 %) < Sit-G (19.0 %). *Table 8* shows calcein leakage from liposomes, and pharmacological bioavailability following intranasal administration of insulin suspension [38] and verapamil powder dosage form with enhancers. Insulin suspension, i.e., insulin-PBS solution containing 1 % SG and Sit-G (18 mM), and 10 % oleic acid (354 mM) was administered to the nasal cavity at a dose of 10 IU/kg in rabbits [38]. Both pharmacological bioavailability of insulin and calcein leakage in 0.5 mM enhancer were increased in the order of oleic acid < SG < Sit-G (*Table 8*). These data suggested that enhancers disturbed the transcellular pathway of the lipid layer in nasal mucosa.

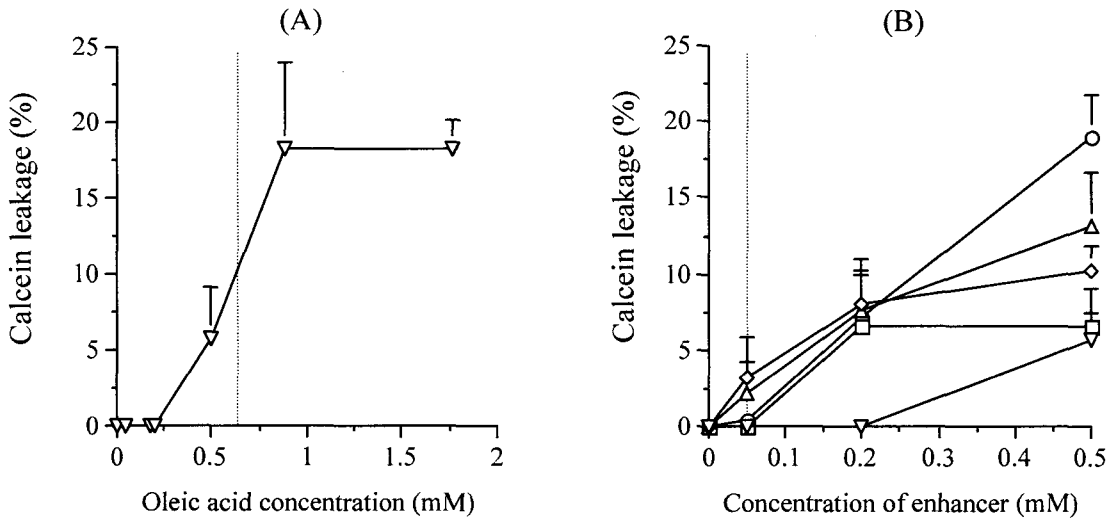

Figure 13. Effect of various enhancers on calcein leakage from liposomes with entrapped calcein in incubation in methanol-1/10 PBS (1:1) at 37 °C for 60 min
(A) Oleic acid, (B) ▽: oleic acid, ◇: SS, □: Sit, △: SG, ○: Sit-G
Hatched line indicates the solubility of each enhancer in a mixture solution of methanol-1/10 PBS (1:1).
Each value represents the mean ± S.D. (n=3-6).
The total lipid concentration was 1.238 μmol/mL.

Table 8. Comparison between calcein leakage from liposomes with entrapped calcein and bioavailability by oleic acid, SG and Sit-G

Enhancer (mM)	Calcein leakage [a] (%)	F (%)	
		Insulin [b]	Verapamil [c]
Oleic acid	5.1 ± 3.4	3.2 ± 1.4	- [d]
SG	13.2 ± 3.6	6.7 ± 1.8	60.4 ± 6.7
Sit-G	19.0 ± 2.9	11.3 ± 1.6	90.7 ± 19.6

Each value represents the mean ± S.D. (n=3-6). * $p < 0.05$, ** $p < 0.01$, *** $p < 0.001$
[a]The enhancer concentration was 0.5 mM and the incubation was at 37 °C for 60 min.
[b]Pharmacological bioavailability (from 0 to 8 hr) of intranasally administered insulin-PBS solution (10 IU/kg) containing 1.0 % SG and Sit-G, and 10 % oleic acid from Ando et. al. [ref. 38]
[c]Bioavailability from 0 to infinity following intranasal administration of verapamil powder containing SG or Sit-G at a dose of 0.75 mg/kg.
[d]No data.

3-4. Change of $[Ca^{2+}]i$ by Sit-G

Paracellular absorption of drugs is restricted by tight junctions. It was reported that the increase in $[Ca^{2+}]i$ was related to the opening of tight junctions [33]. For example, C10 as typical absorption enhancer caused the opening tight junctions via increase in $[Ca^{2+}]i$, and contraction of actomyosin rings [33,53]. On the other hand, ethylendiamine-tetraacetate (EDTA) is also known as an absorption enhancer, but its enhancing mechanism is quite different from C10 since EDTA induced the opening of tight junctions owing to the activation of protein kinase C by the chelation of extracellular calcium ion [33]. Thus, it is the clue for the influence of absorption enhancers on paracellular pathway to estimate the change in calcium ion inside or outside cell. There are no binding sites with calcium ion on the structure of SG and Sit-G and the solubility of these compounds in water is very low, suggesting that SG and Sit-G could not induce the chelation with calcium ion in extracellular sources. Moreover, the efficiency of Sit-G as an enhancer for insulin [38] and verapamil was higher than that of SG. It was considered that the drug absorption was facilitated through the nasal mucosae by SG as the same mechanism as by Sit-G. Therefore, the effects on the paracellular pathway by Sit-G was determined by measuring the changes in $[Ca^{2+}]i$.

Figure14 shows the changes in $[Ca^{2+}]i$ of the excised of nasal mucosae in Ca^{2+} free D-PBS (A) and D-PBS containing 1.4 mM Ca^{2+} (B) after the addition of Sit-G. The addition of 1.4 mM Ca^{2+} and ionomycin rapidly increased $[Ca^{2+}]i$ after the treatment with Sit-G, although the addition of Sit-G did not induced the $[Ca^{2+}]i$ in Ca^{2+} free D-PBS (*Figure 14A*). On the other hand, Sit-G increased $[Ca^{2+}]i$ in D-PBS (*Figure 14B*). These observations suggested that Sit-G did not directly increase $[Ca^{2+}]i$ unlike

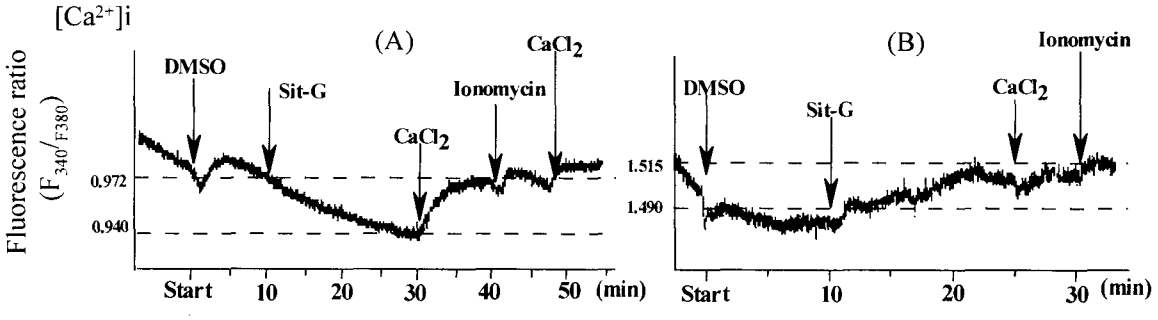

Figure 14. The effect of 50 μM Sit-G on intracellular calcium concentrations in the excised nasal mucosa from rabbits in Ca^{2+} free D-PBS (A), and in D-PBS containing Ca^{2+} (B)
The arrows indicate the time of addition of 1 % DMSO (2 mL), 200 μM Sit-G (50 μL), 200 mM $CaCl_2$ (50 μL), and 26 μM ionomycin (4 mL).
Ordinate axis represents the change of fluorescent intensity ratio of fura PE3 and this change corresponds to that of the intracellular calcium levels.

the effect of C10 [33], but the increase of $[Ca^{2+}]i$ is a secondary factor accompanying alteration of the nasal mucosae by Sit-G. Also, the ionomycin after the addition of Sit-G did not affect the $[Ca^{2+}]i$.

Oleic acid below 0.05 mM increased $[Ca^{2+}]i$ in alveolar cells only in the presence of Ca^{2+} due to the influx of Ca^{2+} from extracellular sources [52], suggesting that the increase of $[Ca^{2+}]i$ is explained by influx of extracellular calcium ions via perturbation of the nasal mucosal membrane by Sit-G. This fact was also explained by the results of calcein leakage from liposomes. As mentioned above, Sit-G induced the perturbation of liposomal membrane from the fact that Sit-G and SG increased the calcein leakage from liposomes entrapped calcein compared with control, Sit and SS. These data suggest that the mechanism of the increase in $[Ca^{2+}]i$ by Sit-G is similar to that of oleic acid. That is, Sit-G may increase the motional freedom of lipids in the mucosal membrane, and facilitated Ca^{2+} influx from extracellular sources. Another possibility is Sit-G may act as an ionophores and make holes as reverse micelles [53]. However, the detailed mechanism of the increase in $[Ca^{2+}]i$ by Sit-G is not clear. Thus, the influence of Sit-G on paracellular pathway was investigated, measuring the change

in TEER and FD-4 permeability.

3-5. Change of TEER and FD-4 permeability by Sit and Sit-G

Figure 15 shows the change in TEER and FD-4 permeability by the addition of enhancers at 1 % w/v to donor side. Ussing chamber system is useful to evaluate the enhancing mechanism of enhancer because of monitoring the TEER and permeated drug through mucosal membrane at the same time. Especially, this method is suitable for evaluation of enhancer on paracellular pathway. As mentioned above, C10 induced the opening of tight junctions due to $[Ca^{2+}]i$, resulting in increase of the drug permeation via paracellular pathway accompanying with a decrease in TEER [32,53]. This result is consistent with the observation shown in *Figure 15*, since C10 caused the increase in FD-4 permeation with decreasing TEER values compared with control.

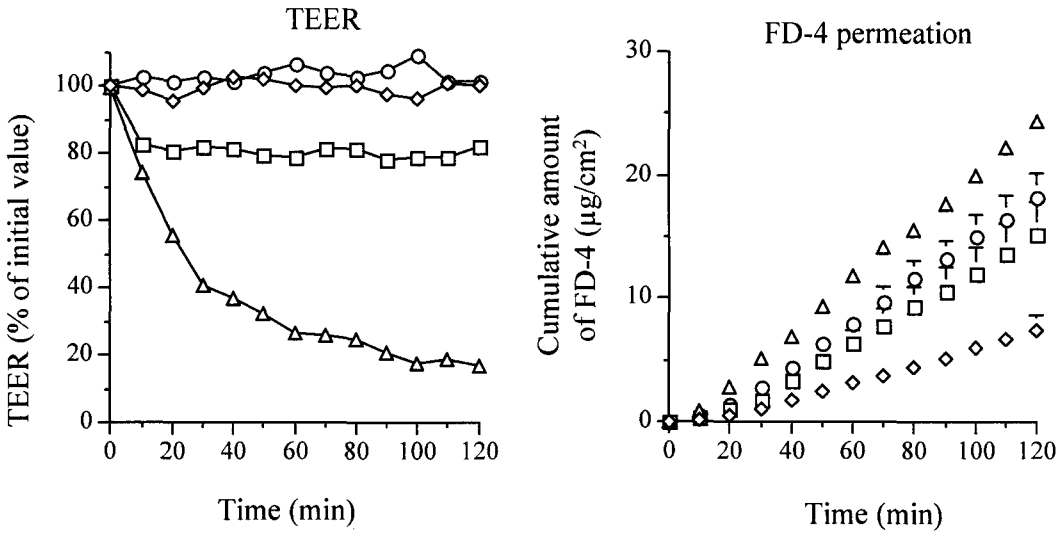

Figure 15. Effects of enhancers on TEER and FD-4 permeation through the excised nasal mucosa in rabbits by the addition of enhancers
◇: control, △: 1 % w/v C 10, □: 1 % w/v Sit suspensions, ○: 1 % w/v Sit-G suspensions
Each value represents the means ± S. E. except for sodium caprate (n=4).
Data for sodium caprate represent means (n=2).

Table 9. Effects of enhancers on TEER and FD-4 permeability *in vitro*

Enhancer	TEER [a] (% of initial value)		*Papp* [b] (x 10^{-6} cm)		*Ef* [c]		
Control [d]	100.5 ± 2.0	*	1.20 ± 0.14	*	1.0	*	**
1 % w/v C10	17.1		5.18		4.3		
1 % w/v Sit	82.2 ± 1.8	*	2.43 ± 0.32	**	2.0 ± 0.3		
1 % w/v Sit-G	101.8 ± 1.3		2.86 ± 0.38		2.9 ± 0.4		

Each value represents the mean ± S.E. (n=4-6).
a) TEER value at 120 min / initial value.
b) Apparent permeation coefficient (*Papp*) was calculated from the following equation
Papp = (dQ/dt)/Co
where dQ/dt is the flux (μg/cm^2), and Co is the initial concentration of FD-4 on the donor side
c) *Ef*; enhancing factor in liquid dosage form = *Papp* enhancer / *Papp* control
d) Control was Ringer's solution containing FD-4.

As shown in *Figure 15 and Table 9*, Sit-G significantly increased *Papp* value without change in TEER value. The increase in $[Ca^{2+}]i$ is insufficient to affect the actin-filaments; therefore, no change was seen in TEER. The results of $[Ca^{2+}]i$ as well as permeation study using Ussing chamber indicate that Sit-G has a little but not bypassed action to the opening of tight junctions. These observations suggested that Sit-G contributes partly to the opening of tight junctions, but it mainly acts in the transcellular pathway. This is also supported from FD-4 transport pathway observed by a confocal laser microscopy. As shown in *Figure 16*, the intracellular fluorescent of FD-4 was partly observed after FD-4 was applied together with Sit-G, although the FD-4 has been reported to be mainly permeated via the paracellular pathway in the nasal mucosae as well as Caco-2 cell. [54,55].

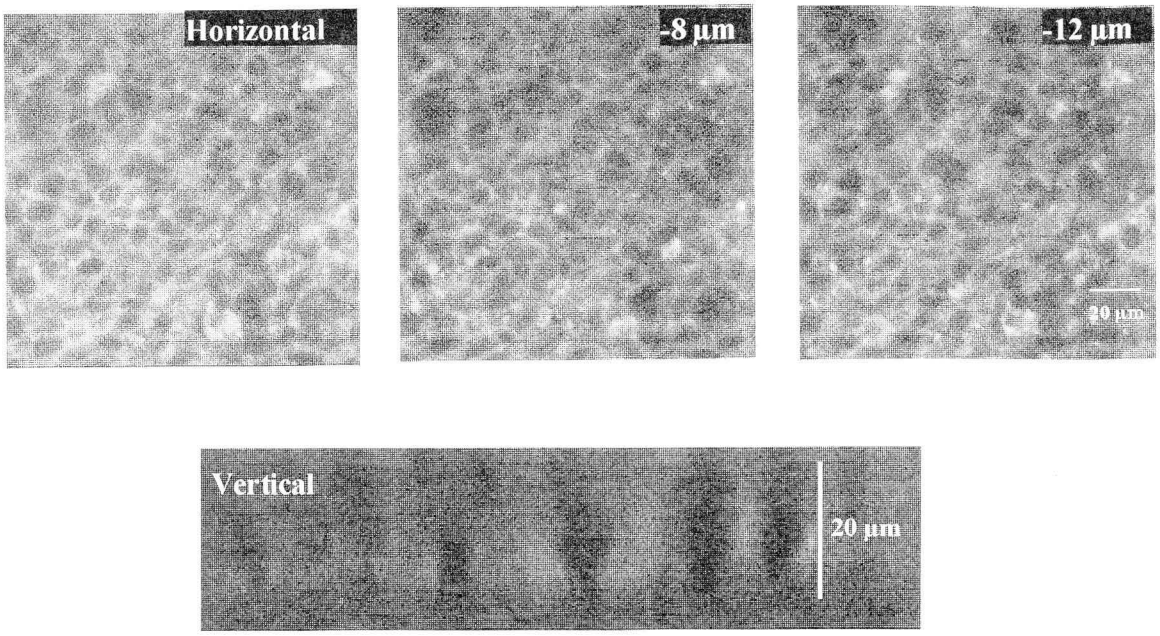

Figure 16. Observation of FD-4 fluorescence on horizontal and vertical cross-sections after permeation study of FD-4 with 1 % w/v Sit-G suspensions for 2 hr across rabbit nasal epithelium by confocal laser scanning microscope
Series of 3 horizontal cross-sections from 0 (horizontal) to -12 μm, taken with steps of 4 μm thickness. Top is apical, bottom is basolateral.

On the other hand, Sit, aglycon of Sit-G, significantly increased *Papp* values compared with control (*Table 9*) and its effect on TEER was different from Sit-G, showing decrease in TEER by 10 min after application of Sit. This finding corresponded well with the observation that Tmax value of FD-4 powder dosage form with Sit *in vivo* was smaller than that with Sit-G. In FD-4 powder dosage form, Sit enhanced the permeation of FD-4 (*Figure 11A*), but did not affect FD-4 uptake into the nasal mucosa compared with control (*Figure 11B*). It has been reported that Sit can substitute for cholesterol in HepG-2 cells [56] and keratinocytes, and it causes transitory perturbation of membranes [57]. In the present study, the uptake of Sit in the nasal mucosae increased compared with that of Sit-G (*Figure 11C*), but the amount of remaining cholesterol was not changed (*data not shown*). These findings suggested

that Sit did not substitute for cholesterol in the nasal mucosa and Sit was rapidly taken up into nasal mucosae after administration of the powder dosage form.

The relationship between *Papp* and AUC values of FD-4 liquid dosage forms, and that between *Papp* and AUC_{TEER} values except for Sit-G were linear (r =0.960, r=0.998), respectively (*Figure 17*). The increase of *Papp* value with Sit and C10 may be involved with a decrease in TEER except for Sit-G. In general, hydrophilic drug permeation through the intracellular space is dependent on the TEER value in the mucosal membrane, which is related to the integrity on the junctional complex. This was supported by the good correlation with a decrease in TEER, and increase of AUC,

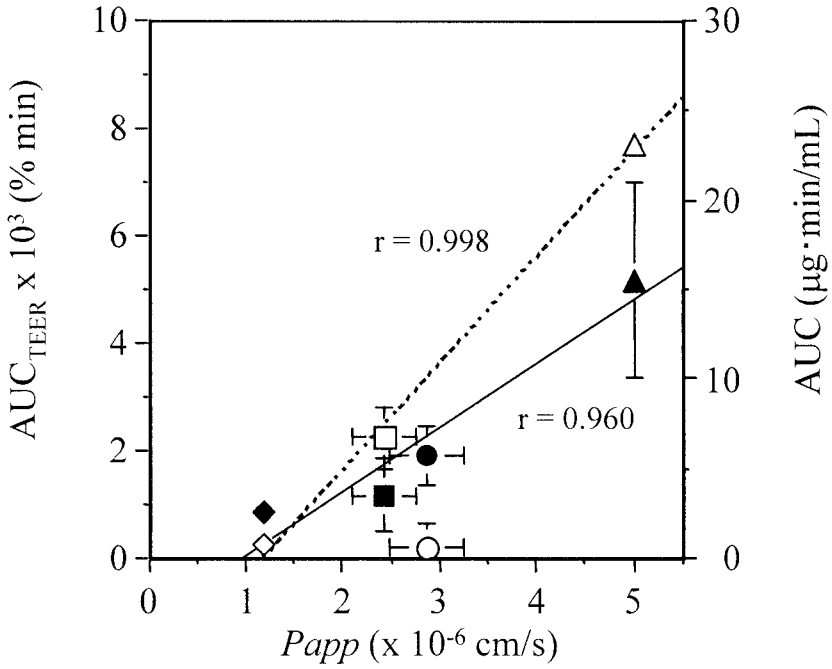

Figure 17. The relationship between Papp, AUC_{TEER} (open symbols) and AUC (closed symbols) values in vivo and in vitro after intranasal administration of FD-4 liquid dosage
◇: control, △: 1 % w/v Sit, □: 1 % w/v Sit-G, ○: 1 % w/v C10
Values of r for the AUC_{TEER} are calculated without the data for Sit-G.
Data represent the mean ± S.E. (n= 4-6).

enhancement factor (*Ef*): i.e., the ratio of F value with enhancer to that with control, vs. *Papp* values (*Figure 17* and *Table 9)*. Sit may loosen the tight junctions, and increase the drug permeation via the paracellular pathway similarly to C10. Thus the enhancement mechanism of Sit-G is different from that of Sit.

The aglycon derivative glycyrrhenic acid was enzymatically produced from glycyrrhizin, and increased drug permeation with a decrease in the TEER value. Thereby, glycyrrhenic acid can enhance drug absorption via the paracellular pathway *in vivo*, however glycyrrhizin did not [58]. The mechanism of enhancement by Sit appears to be similar to that of glycyrrhenic acid, but no such exchange from Sit-G to Sit in nasal mucosae was detected and Sit-G itself showed stronger absorption-enhancing effect than Sit both *in vivo* and *in vitro*. Further, the intracellular calcium levels were reported to be increased by the application of Sit [59]. These findings suggest that the decrease in TEER value by Sit is accompanied by an increase in $[Ca^{2+}]i$, causing the loosening of tight junctions.

The enhancers can be classified into two types based on differences in their mechanism of transport, i.e., paracellular and transcellular types. C10 and EDTA enhanced the drug permeation via paracellular pathway associated with marked decrease in TEER. Palmitoylcarnitine facilitate drug absorption by membrane perturbation effects with a slight increase in the intracellular calcium level (transcellular pathway) [32,37]. This action was observed by the introduction of SG containing Sit-G as the main component into liposomes, which markedly increased the membrane fluidity at 37 °C as determined by measuring electron spin resonance [60]. These findings suggested that the mechanism of action of Sit-G was similar to that of palmitoylcarnitine rather than C10 or EDTA.

The transcellular type enhancers such as Sit-G facilitate drug absorption through the inside of cells; therefore, useful as topical application for gene therapy to increase the introduction of genes into the mucosal cells without irritation of the mucosae.

4. Conclusions

Sit-G increased bioavailability of verapamil, FD-4 and insulin after intranasal administration at the powder dosage form. The enhancing action of Sit-G was higher than that of Sit. As the results of calcein leakage from liposomes as the model of biomembrane after incubation with enhancers, calcein leakage induced by enhancers was in the order of oleic acid < SG < Sit-G. This order was same as that of the enhancement action of bioavailability of verapamil and insulin. Moreover, Sit-G increased $[Ca^{2+}]i$ in the medium containing Ca^{2+}, but did not in Ca^{2+} free medium. With respect to the increase of $[Ca^{2+}]i$, it was considered that the Ca^{2+} influx was induced by Sit-G due to the perturbation of mucosal membrane, or Sit-G acted as ionophores and made holes as reverse micelles on the mucosal membrane.

However, the increase of $[Ca^{2+}]i$ dose not relate to the opening of tight junctions since Sit-G increases the FD-4 permeability through the excised rabbit nasal mucosa without decrease of TEER. These findings suggested that Sit-G might enhance the

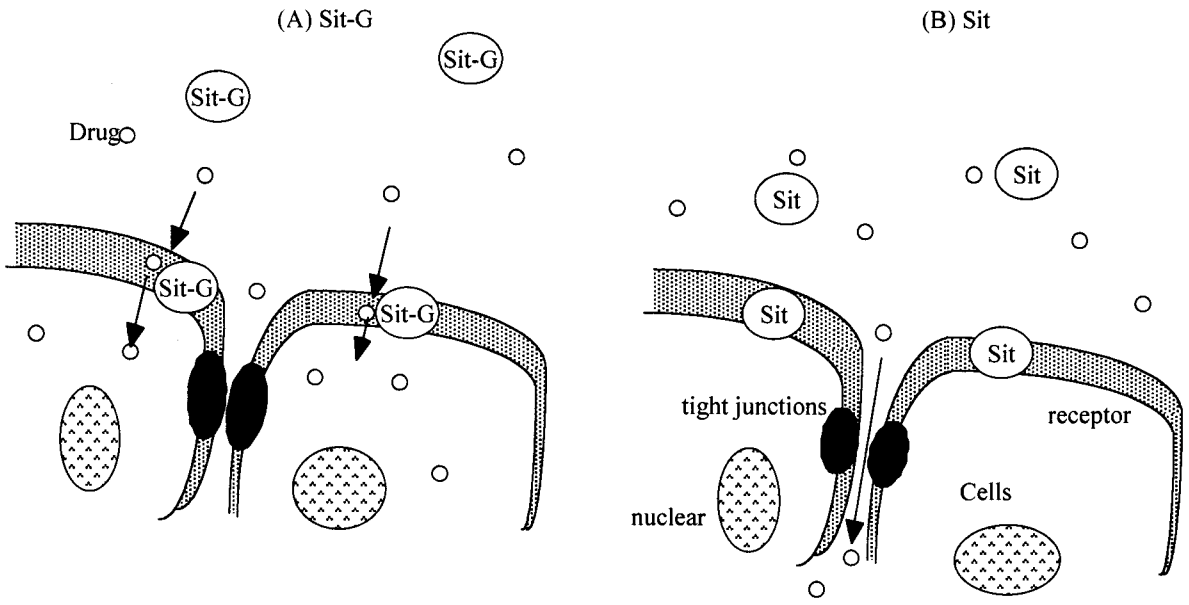

Figure 18. Absorption enhancing mechanism of Sit-G and Sit after intranasal administration of dosage forms with Sit-G (A) and Sit (B)

drug absorption via the transcellular pathway due to perturbation of mucosal membrane (*Figure 18*), and this is also supported by the observation of FD-4 transport pathway by confocal laser microscopy, which showed that the fluorescence of FD-4 was widely distributed except in goblet cells. On the other hand, Sit contributes mainly the opening of tight junctions (*Figure 18*) as an increase in FD-4 permeation along with a decrease in TEER was seen by the application of this compound.

Chapter III

Effect of Nanoparticle Based on β-Sitosterol β-D-Glucoside and β-Sitosterol on Intranasal Absorption of FITC-Dextran 4,400

1. Introduction

As described in *Chapter II*, Sit and Sit-G enhanced effectively the drug absorption across the nasal mucosa, and the enhancement mechanism of these enhancers was elucidated by various *in vitro* experiments. One of the shortcomings of these enhancers is a poor dispersibility in water due to their high hydrophobicity. This restricts the administered dosage form, resulting in a limitation of the enhancing ability. In the dispersions of Sit and Sit-G powders (< 75 μm), most of them floated at the surface of water. To solve the poor dispersibility of Sit and Sit-G in water, the NP composed of Sit and Sit-G were developed (Sit and Sit-G NP). The aim in *Chapter III* was to evaluate the enhancing effect of Sit and Sit-G NP *in vivo* and *in vitro*, and to elucidate the mechanism of enhancement in comparison with Sit and Sit-G suspensions.

2. Experimental Section

2-1. Materials

Sit, Sit-G, FD-4 and C10 were the same ones in Chapter II. Phloridzin (PHZ), was purchased from Sigma Chemical (St. Louis, MO). Sodium oleate was purchased from Tokyo Kasei Kogyo (Tokyo, Japan). All other chemicals used were of analytical reagent grade.

2-2. Preparation of dosage form

For preparation of suspension, the powder of enhancers sieved with 200 mesh (75 μm, SP) was dispersed into PBS and prepared by sonication (SP suspension). Sit and Sit-G NP was prepared by the modified ethanol injection method [11]. Briefly, 10 mg Sit or Sit-G, and 50 mg sodium oleate were dissolved in hot ethanol 60 °C, and then 20 mL of PBS was added. Ethanol was removed from the resultant 0.05 % w/v NP suspension. The size and polydispersity index of prepared NP was about 80 nm and less than 0.25, respectively (*Figure 19*). FD-4 was dissolved in the SP and NP to the

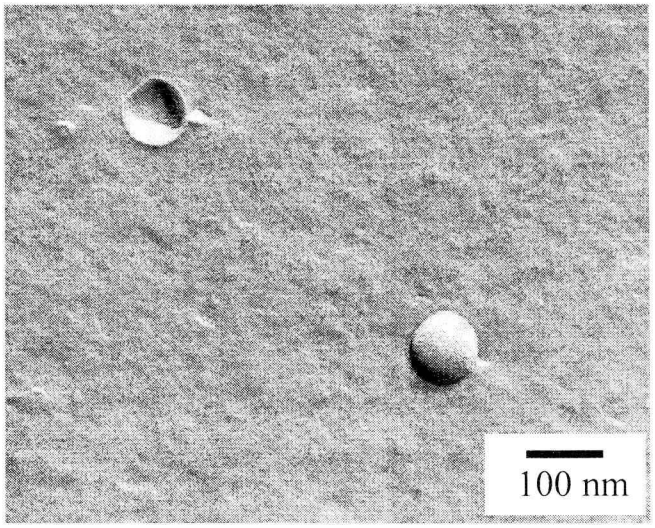

Figure 19. Observation of Sit-G nanoparticles by freeze fracture (magnification x 100,000)

required concentration, respectively.

2-3. Animal experiment

Aliquot of 50 μL each liquid dosage form were administered via nostril of Japanese white rabbits (about 2 kg, Sankyo Laboratory, Japan) restrained in the supine position for 5 min at a dose of 1 mg/kg FD-4. At each time point, the blood samples were taken from ear vein until 8 hr. Plasma concentration, F value and absorption constant rate (Ka) values were determined by the method described in *Chapter II.* AUC of FD-4 from time 0 to 8 hr was estimated from the sum of successive trapezoids between each data point.

2-4. Measurement of FD-4 and TEER in the Ussing chamber

The experimental methods were described in *Chapter II.* Briefly, The excised nasal mucosa was mounted onto a tissue adapter in an Ussing chamber (CEZ-9100, Nihon Kohden, Tokyo, Japan). Each chamber was filled with Ringer's solution. Temperature was kept constant at 37 °C by a water jacket. After preincubation for 1 hr, 0.05 % w/v C10 solution, and Sit and Sit-G SP, and Sit and Sit-G NP was added to the donor side. For inhibition study of glucose/Na^+ cotransporter using PHZ, PHZ was added to the donor side. Samples and TEER were taken from receiver side, and measured at every 10 min up to 120 min.

2-5. Data analysis

The data analysis was carried out by the method mentioned in *Chapter I.*

3. Results and Discussion

3-1. Effects of SP and NP on intranasal absorption of FD-4

From the gel-filtration of FD-4 and NP (NP dosage from), FD-4 was not housed in NP (*data not shown*). *Figure 20* shows the plasma concentration profiles of FD-4 following intranasal administration of Sit and Sit-G SP and NP at a dose of 1 mg FD-4/kg in rabbits. Sodium oleate at 0.25 % w/v was control as the NP dosage form. C10 was used as the active control since it is widely used as the absorption enhancer. *Table 10* summarized the bioavailability, Ka, and *Papp* values. Sodium oleate did not affect FD-4 absorption through nasal mucosa since no significant difference on the bioavailability of FD-4 was observed between sodium oleate and PBS control ($p > 0.05$). This finding suggested that enhancement of FD-4 absorption by both NP was not due to

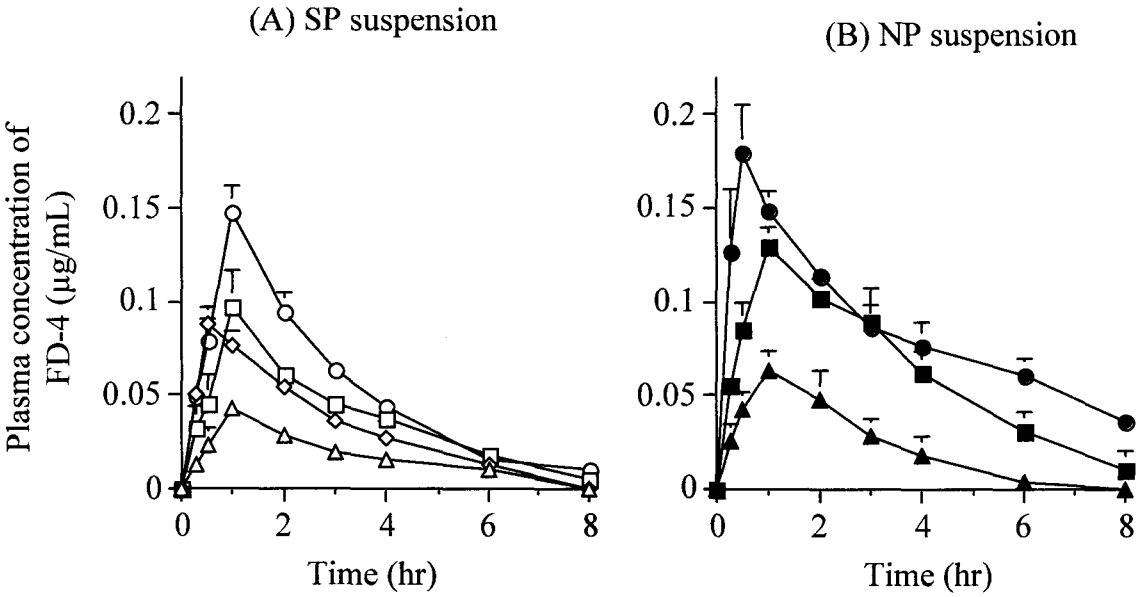

Figure 20. Plasma concentration profile of FD-4 following intranasal administration of liquid dosage forms in rabbits at a dose of 1 mg FD-4/kg
(A) SP suspension △: PBS, ◇: 0.05% (w/v) C 10, □: 0.05% w/v Sit SP, ○: 0.05% w/v Sit-G SP
(B) NP suspension; ▲: 0.25 % w/v sodium oleate (control of NP), ■: 0.05% w/v Sit NP, ●: 0.05% w/v Sit-G NP
Each value represents the mean ± S.E. (n=4-6).

sodium oleate but to Sit or Sit-G. Sit and Sit-G NP showed significantly 3.8- and 5.1-fold higher bioavailability than PBS control, and 1.8- and 1.7-fold higher than Sit and Sit-G SP, respectively. Sit-G enhanced the FD-4 absorption compared with Sit in NP and SP, respectively. Ka values of Sit-G NP significantly increased compared with Sit (*Table 10*). Thus, NP was more effective form than SP, and Sit-G NP was more effective than that of Sit NP.

Table 10. Bioavailability and absorption rate constant (Ka) value of FD-4 following intranasal administration of FD-4 with each liquid dosage form at a dose of 1 mg FD-4/kg in rabbits, and permeability coefficient (*Papp*) of FD-4 according to permeation study in vitro at 0.05% w/v enhancer

Enhancer	F [a)] (%)	Ka (hr^{-1})	*Papp* [b)] (x 10^{-6} cm)
Solution			
PBS	4.0 ± 0.8	1.11 ± 0.09	1.20 ± 0.35
Sodium oelate	4.6 ± 1.0	1.01 ± 0.12	- [c)]
C10	7.3 ± 0.7	3.63 ± 0.46	5.18
Suspension			
Sit	8.7 ± 1.1	1.09 ± 0.13	1.61 ± 0.40
Sit-G	12.0 ± 0.6	1.36 ± 0.21	3.71 ± 0.94
Nanoparticle			
Sit	15.3 ± 2.2	1.82 ± 0.47	1.23 ± 0.28
Sit-G	20.2 ± 0.9	6.18 ± 0.76	2.84 ± 0.87
Sit-G + PHZ	- [c)]	- [c)]	3.18 ± 1.20

Each value in intranasal administration and permeation study is represented as the mean ± S.E. and S.D., respectively. (n=4)
* $p < 0.05$, ** $p < 0.01$
a) F (from 0 to 8 hr)
b) *Papp* = $(dQ/dt)/(C_0 \times A)$
where dQ/dt is the flux (mg/cm^2), C_0 is the initial concentration of FD-4 in donor side and A is the surface area.
c) Not determined

3-2. Influence of SP and NP on TEER and FD-4 permeation

Sit-G NP, Sit-G and Sit SP, and C10 solution increased significantly *Papp* values compared with control, while Sit-G NP and Sit SP significantly decreased TEER by

70 % at 10 min, returning to 90 % by 30 min, and kept a significant decrease similar to C10, respectively (*Figure 21* and *Table 10*). The decrease of TEER induced by Sit-G NP was diminished by the addition of the specific substrate of the glucose/Na^+ cotransporter PHZ at 1 mM [61] to the donor side (*Figure 21*), but no change of *Papp* values was seen (*Table 10*). Sit-G NP may have affinity to the glucose/Na^+ cotransporter, resulting in a decrease of TEER, but such phenomenon was not seen in the case of Sit-G SP. The glucose residue of Sit-G is recognized more readily by the glucose/Na^+ cotransporter in the form of NP than in SP.

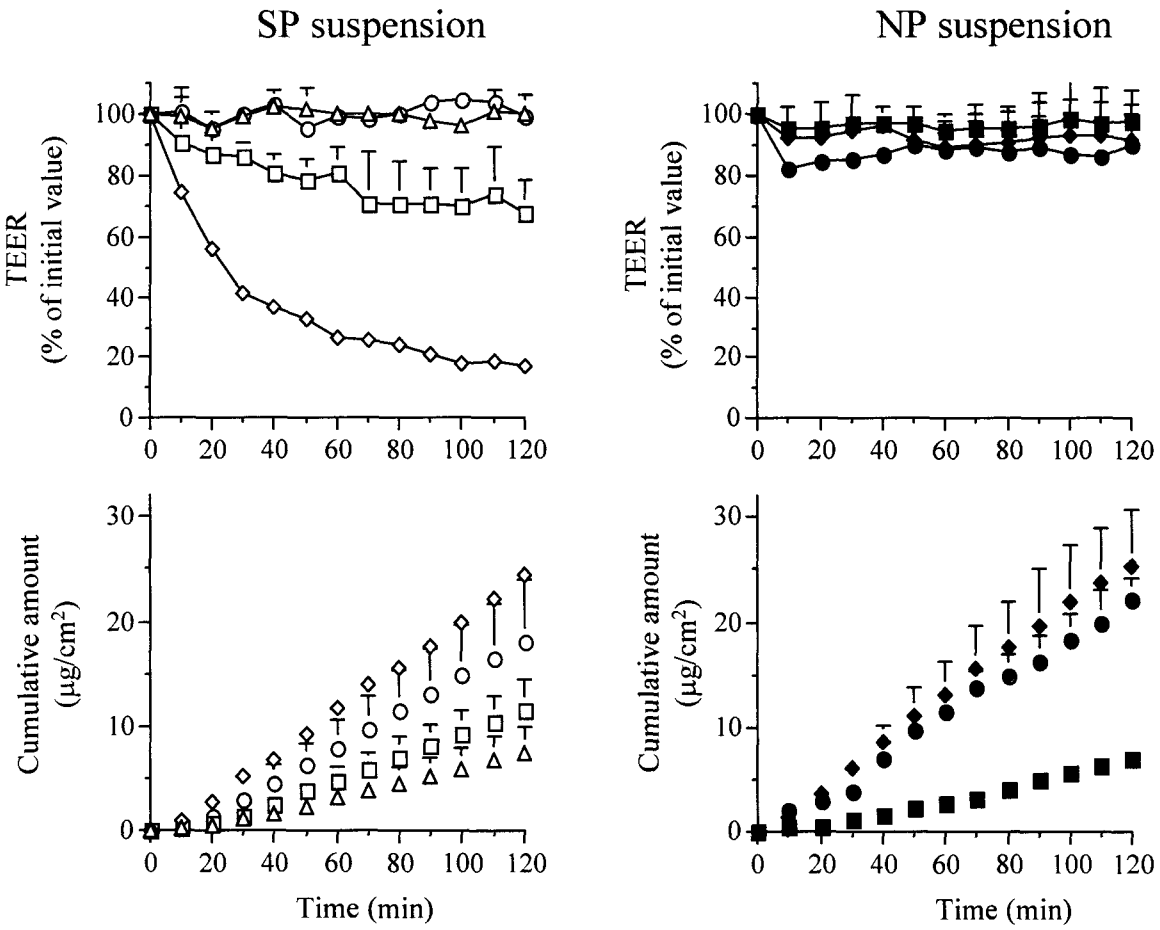

Figure 21. Effects of enhancers on TEER and FD-4 permeation through the excised nasal mucosa in rabbits by the addition of enhancers
△: control, ◇: 0.05 % w/v C10, □: 0.05 % w/v Sit SP, ○: 0.05 % w/v Sit-G SP
■: 0.05% w/v Sit NP, ●: 0.05% w/v Sit-G NP, ◆: 0.05% w/v Sit-G NP + 1 mM PHZ
Each value represents the means ± S.E. except for sodium caprate (n=4).
Data for sodium caprate represent means (n=2).

4. Conclusions

Co-administration of Sit or Sit-G NP with FD-4 in nasal mucosa significantly increased bioavailability. Sit-G NP is readily recognized by the glucose/Na^+ cotransporter unlike Sit-G SP. Sit and Sit-G NP might interact with nasal mucosa compared with their SP due to the small particle size and providing the uniformly dispersion in nasal fluid. NP incorporated Sit and Sit-G are potential dosage forms as a nasal delivery for a hydrophilic and high molecular weight drug such as FD-4.

SUMMARY

The nasal absorption has received an increased attention especially in improving the delivery of peptide drugs. In this thesis, I have used bioadhesive polymers as drug carriers, absorption enhancers and nanoparticle dosage forms to a control of drug release and to increase bioavailabilities for nasal drug delivery. Drug release from the drug-loaded polymers exhibited classical Fickian kinetics after an initial burst, and the system was evaluated using nasal rabbits to confirm whether these polymer-gels could effectively deliver the drug in physiological conditions, such as nasal mucosa.

As described in *Chapter II* and *III*, Sit-G and Sit significantly facilitated the absorption of verapamil and FD-4 as well as insulin following intranasal administration of the powder, liquid and nanoparticle dosage forms. It was evident that Sit-G exhibited the stronger absorption activity (*Table 11*). Absorption enhancers are classified into two groups; the paracellular and transcellular types. Most of enhancers are involved in the former type, which looses the tight junctions via various mechanisms, i.e., i) increase in the intracellular calcium levels, ii) depletion of calcium ion in tight junctions. Results of mechanistic study of Sit-G revealed that the behavior of transepithelial resistance (TEER) was not consistent with the observation of paracellular type enhancer such as sodium caprate, EDTA and chitosan. Sit-G increased the permeability of drug across the excised nasal mucosa without a decrease in TEER value, although Sit increased it accompanying with a decrease in TEER. The decrease of TEER value means the increase of ion transport from the mucosal to serosal side, close relating to the opening of tight junctions. These findings suggested that Sit-G did not act in the paracellular pathway. To estimate influence of Sit-G on mucosal membrane, liposomes entrapped

Table 11. Bioavailability of various dosage form of insulin, verapamil and FD-4 formulae with enhancers following intranasal administration in rabbits

Drug	Dose	Formulation	Enhancer	F [a] (%)
Insulin	10 IU/kg	Suspension [b]	10 % w/v oleic acid	3.2 ± 1.4
			1 % w/v SG	6.7 ± 1.4
			1 % w/v Sit-G	11.3 ± 1.6
Verapamil	0.75 mg/kg	Powder [c]	Lactose (control)	39.8 ± 3.4
			SG	60.4 ± 3.5
			Sit-G	90.7 ± 9.8
FD-4	1 mg/kg	Powder [d]	Lactose (control)	4.1 ± 1.1
			Sit	6.9 ± 0.4
			Sit-G	8.3 ± 1.0
		Solution	PBS (cotnrol)	2.6 ± 0.4
			0.05 % w/v C10	5.6 ± 0.3
			1.0 % w/v C10	8.2 ± 2.9
		Suspension SP [b]	0.05 % w/v Sit	5.8 ± 0.9
			0.05 % w/v Sit-G	8.9 ± 0.4
		NP [e]	0.05 % w/v Sit	9.2 ± 0.8
			0.05 % w/v Sit-G	11.7 ± 0.7

a) F from 0 to 8 hr for insulin, F from 0 to infinity for verapamil and F from 0 to 3 hr for FD-4.
b) Particles are less than 75 μm.
c) verapamil:enhancers = 1:3 weight
d) FD-4:enhancer = 1:2 weight
e) The size of nanoparticle is about 80 nm.

calcein were incubated with enhancers. Sit-G induced the calcein leakage, but Sit did not, suggesting that Sit-G perturbs mucosal membranes, thereby, drug absorption increased via transcellular pathway. On the contrary, Sit facilitates drug absorption via paracellular pathway.

While Sit-G and Sit are useful as an enhancer, they are scarcely soluble in water. In order to solve this drawback, preparation of nanoparticle based on Sit and Sit-G was investigated. The success of the preparation of nanoparticles resulted in the preferable dosage form for nasal delivery with an enhancer of Sit or Sit-G. Sit and Sit-G nanoparticles significantly enhanced FD-4 absorption following an intranasal

administration of FD-4. Especially, Sit-G nanoparticle showed the greatest activity among other dosage forms.

Modulation of the gel swelling and mucoadhesiveness may prove usefulness in the controlled release of drug from pH-sensitive and adhesive polymer at the surface of the nasal mucosa *in vivo*. For the poor absorbable drugs across nasal mucosae, Sit-G is a useful transcellular type enhancer in nasal absorption of drugs. Furthermore, Sit-G nanoparticles may be applicable as an enhancer in the intestinal, or other mucosal delivery.

In conclusion, nasal administration of drugs, especially peptides, along with bioadhesive polymers or nanoparticle dosage forms in combination with nontoxic enhancer, i.e., Sit-G provides a promising method as an alternative for the injection.

ACKNOWLEDGMENTS

First, I would like to express my gratitude and appreciation from my heat to professor Kozo Takayama and Emeritus Professor and President Hoshi University Tsuneji Nagai for their helpful guidance in my research work and preparing this dissertation.

Secondary, I would like to thank Professor Nicholaos A. Peppas (Department of chemical Engineering, Purdue University) and Associate Professor Anthony M Lowman (Chemical Engineering Department, Drexel University) for providing me polymer and great suggestion about polymer study.

Further, I wish to thank Associate Professor Yoshie Maitani for the greatest help in my research work, showing me the way of researcher.

Moreover, I would like to thank Associate Professor Nobuko Sakurai, Professor Katsuo Kamata, and Mr. Hiroshi Suenaga for the suggestion in my research.

Also, I wish to thank Dr. Mariko Morishita and Dr. Yasuko Obata and all my colleagues of the Department of Pharmaceutics for their friendship and the relaxing moments I lived during this period.

In addition, I would like to thank Ms. Chie Ichihara, Ms. Shiho Yamagata, Ms. Yasuko Oka, Mr. Takahiro Nagamoto, Ms. Mai Tamura, and Ms. Sayaka Ishijima for assistant in my research.

To people of the library and the office for their helpful attention.

Finally, I will be forever dept to my fondest parents for their words and comprehension.

REFERENCES

[1] Banga AK, Chien YW. Systemic delivery of therapeutic peptides and proteins. *Int J Pharm*, 1988, **48**, 15-50.

[2] Donovan MD, Flynn GL, Amidon GL. The molecular weight dependence of nasal absorption: the effect of absorption enhancers. *Pharm Res*, 1990, **7**, 808-815.

[3] McMartin C, Hutchinson LE, Hyde R, Peters GE. Analysis of structural requirements for the absorption of drugs and macromolecules from the nasal cavity. *J Pharm Sci*, 1987, **76**, 535-540.

[4] Yamamoto A, Morita T, Hashida M, Sezaki H. Effect of absorption promoters on the nasal absosrption of drugs with various molecular weights. *Int J Pharm*, 1993, **93**, 91-99.

[5] Kan CC, Bittman R. Spontaneous rates of sitosterol and cholesterol exchange between phospholipid besicles and between lysophospholipid dispersions: Evidence that desorption rate is impeded by the 24a-ethly group of sitosterol. *J Am Chem Soc*, 1991, **113**, 6650-6656.

[6] Compassi S, Werder M, Weber FE, Boffelli D, Hauser H, Schulthess G. Comparison of cholesterol and sitosterol uptake in different brush border membrane models. *Biochemistry*, 1997, **36**, 6643-6652.

[7] von Holtz RL, Fink CS, Awad AB. beta-Sitosterol activates the sphingomyelin cycle and induces apoptosis in LNCaP human prostate cancer cells. *Nutr Cancer*, 1998, **32**, 8-12.

[8] Awad AB, von Holtz RL, Cone JP, Fink CS, Chen YC. beta-Sitosterol inhibits growth of HT-29 human colon cancer cells by activating the sphingomyelin cycle. *Anticancer Res*, 1998, **18**, 471-473.

[9] Raicht RF, Cohen BI, Fazzini EP, Sarwal AN, Takahashi M. Protective effect of plant sterols against chemically induced colon tumors in rats. *Cancer Res*, 1980, **40**, 403-405.

[10] Shimizu K, Maitani Y, Takahashi N, Takayama K, Nagai T. Association of liposomes containing a soybean-derived sterylglucoside mixture with rat primary cultured hepatocytes. *Biol Pharm Bull*, 1998, **21**, 818-22.

[11] Maitani Y, Soeda H, Jumping W, Takayama K. Modified ethanol injection method for liposome containing β-sitosterol β-D-glucoside. *J Liposome Res*, 2001, **11**, 115-125.

[12] Ivorra MD, Paya M, Villar A. Effect of beta-sitosterol-3-beta-D-glucoside on insulin secretion in vivo in diabetic rats and in vitro in isolated rat islets of Langerhans. *Pharmazie*, 1990, **45**, 271-273.

[13] Maitani Y, Yamamoto T, Takayama K, Nagai T. The effect of soybean-derived sterol and its glucoside as an enhancer of nasal absorption of insulin in rabbits in vitro and in vivo. *Int J Pharm*, 1995, **117**, 129-137.

[14] Yamamoto T, Maitani Y, Ando T, Isowa K, Takayama K, Nagai T. High absorbency and subchronic morphologic effects on the nasal epithelium of a nasal insulin powder dosage form with a soybean-derived sterylglucoside mixture in rabbits. *Biol Pharm Bull*, 1998, **21**, 866-870.

[15] Aikawa K, Mitsutake N, Uda H, Tanaka S, Shimamura H, Aramaki Y, Tsuchiya S. Drug release from pH-response polyvinylacetal diethylaminoacetate hydrogel, and application to nasal delivery. *Int J Pharm*, 1998, **168**, 181-188.

[16] Lowman AM, Peppas NA. Analysis of the complexation/decomplexation phenomena in graft copolymer networks. *Maclomolecules*, 1997, **30**, 4959-4965.

[17]Lowman AM, Peppas NA, Morishita M, Nagai T. Novel bioadhesive complexation networks for oral protein delivery. Tailored Polymeric Materials for Controlled Drug Delivery Systems, ACS Symposium Series, Vol. 709, Washington, DC, 1998, pp. 156-164.

[18]Ryrfeldt A, Andersson P, Edsbacker S, Tonnesson M, Davies D, Pauwels R. Pharmacokinetics and metabolism of budesonide, a selective glucocorticoid. *Eur J Respir Dis Suppl*, 1982, **122**, 86-95.

[19]Roth G, Wikby A, Nilsson L, Thalen A. High-performance liquid chromatographic determination of epimers, impurities, and content of the glucocorticoid budesonide and preparation of primary standard. *J Pharm Sci*, 1980, **69**, 766-770.

[20]Maitani Y, Igawa T, Machida Y, Nagai T. Plasma levels following intranasal and intravenous administration of human interferon-beta to rabbits. *Drug Des Deliv*, 1989, **4**, 109-119.

[21]Yamaoka K, Tanigawara Y, Nakagawa T, Uno T. A pharmacokinetic analysis program (MULTI) for microcomputers. *J Pharma Dyn*, 1981, **4**, 879-885.

[22]Falk R, Randolph TW, Meyer JD, Kelly RM, Manning MC. Controlled release of ionic compound from poly (L-lactide) microspheres produced by precipitation with a compressed antisolvent. *J Control Release*, 1997, **44**, 77-85.

[23]Aspden TJ, Mason JD, Jones NS, Lowe J, Skaugrud O, Illum L. Chitosan as a nasal delivery system: the effect of chitosan solutions on in vitro and in vivo mucociliary transport rates in human turbinates and volunteers. *J Pharm Sci*, 1997, **86**, 509-513.

[24]Mortazavi SA. An in vitro assessment of mucus/mucoadhesive interactions. *Int J Pharm*, 1995, **124**, 173-182.

[25]Wuthrich P, Martenet M, Buri P. Effect of formulation additives upon the intranasal

bioavailability of a peptide drug: tetracosactide ($ACTH_{1-24}$). *Pharm Res*, 1994, **11**, 278-282.

[26]Abe K, Irie T, Uekama K. Enhanced nasal delivery of luteinizing hormone releasing hormone agonist buserelin by oleic acid solubilized and stabilized in hydroxypropyl-beta-cyclodextrin. *Chem Pharm Bull*, 1995, **43**, 2232-2237.

[27]Pillion DJ, Recchia J, Wang P, Marciani DJ, Kensil CR. DS-1, a modified Quillaja saponin, enhances ocular and nasal absorption of insulin. *J Pharm Sci*, 1995, **84**, 1276-1279.

[28]Merkus FWHM, Verhoef JC, Romeijn SG, Schipper NGM. Absorption enhancing effect of cyclodextrins on intranasally administered insulin in rats. *Pharm Res*, 1991, **8**, 588-592.

[29]Marttin E, Verhoef JC, Romeijn SG, Merkus FWHM. Effects of absorption enhancers on rat nasal epithelium in vivo: release of marker compounds in the nasal cavity. *Pharm Res*, 1995, **12**, 1151-1157.

[30]Arnold TH, Tackett RL, Vallner JJ. Pharmacodynamics of acute intranasal administration of verapamil: comparison with i.v. and oral administration. *Biopharm Drug Dispos*, 1985, **6**, 447-454.

[31]Noach AB, Kurosaki Y, Blom-Roosemalen MCM, de Boer AG, Breimer DD. Cell-polarity dependent effect of chelation on the paracellular permeability of conluent Caco-2 cell monolayers. *Int J Pharm*, 1993, **90**, 229-237.

[32]Tomita M, Hayashi M, Awazu S. Absorption-enhancing mechanism of sodium caprate and decanoylcarnitine in Caco-2 cells. *J Pharmacol Exp Ther*, 1995, **272**, 739-743.

[33]Tomita M, Hayashi M, Awazu S. Absorption-enhancing mechanism of EDTA,

caprate, and decanoylcarnitine in Caco-2 cells. *J Pharm Sci*, 1996, **85**, 608-611.

[34]Morita T, Yamamoto A, Hashida M, Sezaki H. Effects of various absorption promoters on pulmonary absorption of drugs with different molecular weights. *Biol Pharm Bull*, 1993, **16**, 259-262.

[35]El-Shafy MA, Kellaway IW, Taylor G, Dickinson PA. Improved nasal bioavailability of FITC-dextran (Mw 4300) from mucoadhesive microspheres in rabbits. *J Drug Target*, 2000, **7**, 355-361.

[36]Junginger HE, Hoogstraate JA, Verhoef JC. Recent advances in buccal drug delivery and absorption--in vitro and in vivo studies. *J Control Release*, 1999, **62**, 149-159.

[37]LeCluyse EL, Appel LE, Sutton SC. Relationship between drug absorption enhancing activity and membrane perturbing effects of acylcarnitines. *Pharm Res*, 1991, **8**, 84-87.

[38]Ando T, Maitani Y, Yamamoto T, Takayama K, Nagai T. Nasal insulin delivery in rabbits using soybean-derived sterylglucoside and sterol mixtures as novel enhancers in suspension dosage forms. *Biol Pharm Bull*, 1998, **21**, 862-865.

[39]Christrup LL, Bonde J, Rasmussen SN, Rassing MR. Relative bioavailability of (+/-)-verapamil hydrochloride administered in tablets and chewing gum. *Acta Pharm Nord*, 1990, **2**, 371-376.

[40]Szoka F, Papahadjopoulos D. Procedure for preparation of liposomes with large internal aqueous space and high capture by reverse-reverse phase evaporation. *Proc Narl Acad Sci USA*, 1978, **75**, 4194-4198.

[41]Qi XR, Maitani Y, Nagai T. Effect of soybean-derived sterols on the in vitro stability and the blood circulation of liposomes in mice. *Int J Pharm*, 1995, **114**,

33-41.

[42]Mishima M, Wakita Y, Nakano M. Studies on the promoting effects of medium chain fatty acid salts on the nasal absorption of insulin in rats. *J Pharmcobiodyn*, 1987, **10**, 624-631.

[43]Sugimoto K, Yoshida M, Yata T, Higaki K, Kimura T. Evaluation of poly(vinyl alcohol)-gel spheres containing chitosan as dosage form to control gastrointestinal transit time of drugs. *Biol Pharm Bull*, 1998, **21**, 1202-1206.

[44]Shimazaki T, Tomita M, Sadahiro S, Hayashi M, Awazu S. Absorption-enhancing effects of sodium caprate and palmitoyl carnitine in rat and human colons. *Dig Dis Sci*, 1998, **43**, 641-645.

[45]Lindmark T, Schipper N, Lazorova L, de Boer AG, Artursson P. Absorption enhancement in intestinal epithelial Caco-2 monolayers by sodium caprate: assessment of molecular weight dependence and demonstration of transport routes. *J Drug Target*, 1998, **5**, 215-223.

[46]Custodio JB, Almeida LM, Madeira VM. The anticancer drug tamoxifen induces changes in the physical properties of model and native membranes. *Biochim Biophys Acta*, 1993, **1150**, 123-129.

[47]Muramatsu K, Maitani Y, Machida Y, Nagai T. Effect of soybean-derived sterol and its glucoside on the stability of diplamitoylphosphatidylcholine and dipalmitoylphosphatidylcholine/cholesterol liposomes. *Int J Pharm*, 1994, **107**, 1-8.

[48]Schuler I, Duportail G, Glasser N, Benveniste P, Hartmann MA. Soybean phosphatidylcholine vesicles containing plant sterols: a fluorescence anisotropy study. *Biochim Biophys Acta*, 1990, **1028**, 82-88.

[49]Slotte JP, Jungner M, Vilcheze C, Bittman R. Effect of sterol side-chain structure

on sterol-phosphatidylcholine interactions in monolayers and small unilamellar vesicles. *Biochim Biophys Acta*, 1994, **1190**, 435-443.

[50] Suzuki A, Morishita M, Kajita M, Takayama K, Isowa K, Chiba Y, Tokiwa S, Nagai T. Enhanced colonic and rectal absorption of insulin using a multiple emulsion containing eicosapentaenoic acid and docosahexaenoic acid. *J Pharm Sci*, 1998, **87**, 1196-1202.

[51] Tsutsumi K, Obata Y, Takayama K, Loftsson T, Nagai T. Effect of the cod-liver extract on the buccal permeation of ionized and nonionized forms of ergotamine using the keratinized epithelial-free membrane of hamster cheek pouch mucosa. *Int J Pharm*, 1998, **174**, 151-156.

[52] Wang LY, Ma JK, Pan WF, Toledo-Velasquez D, Malanga CJ, Rojanasakul Y. Alveolar permeability enhancement by oleic acid and related fatty acids: evidence for a calcium-dependent mechanism. *Pharm Res*, 1994, **11**, 513-517.

[53] Sakai M, Imai T, Ohtake H, Azuma H, Otagiri M. Effects of absorption enhancers on cytoskeletal actin filaments in Caco-2 cell monolayers. *Life Sci*, 1998, **63**, 45-54.

[54] Marttin E, Verhoef JC, Cullander C, Romeijn SG, Nagelkerke JF, Merkus FW. Confocal laser scanning microscopic visualization of the transport of dextrans after nasal administration to rats: effects of absorption enhancers. *Pharm Res*, 1997, **14**, 631-637.

[55] Schipper NG, Olsson S, Hoogstraate JA, deBoer AG, Varum KM, Artursson P. Chitosans as absorption enhancers for poorly absorbable drugs 2: mechanism of absorption enhancement. *Pharm Res*, 1997, **14**, 923-929.

[56] Bhadra S, Subbiah MT. Incorporation of liposomal phytosterols into human cells in culture: a potential in vitro model for investigating pathological effects of

phytosterolemia. *Biochem Med Metab Biol*, 1991, **46**, 119-124.

[57] Mora MP, Tourne-Peteilh C, Charveron M, Fabre B, Milon A, Muller I. Optimisation of plant sterols incorporation in human keratinocyte plasma membrane and modulation of membrane fluidity. *Chem Phys Lipids*, 1999, **101**, 255-265.

[58] Imai T, Sakai M, Ohtake H, Azuma H, Otagiri M. In vitro and in vivo evaluation of the enhancing activity of glycyrrhizin on the intestinal absorption of drugs. *Pharm Res*, 1999, **16**, 80-86.

[59] Hennessey TM. Effects of membrane plant sterol on excitable cell functions. *Comp Biochem Physiol*, 1992, **101C**, 1-8.

[60] Muramatsu K, Masumizu T, Maitani Y, Hwang SH, Kohno M, Takayama K, Nagai T. Electron spin resonance studies of dipalmitoylphosphatidylcholine liposomes containing soybean-derived sterylglucoside. *Chem Pharm Bull*, 2000, **48**, 610-613.

[61] Atisook K, Carlson S, Madara JL. Effects of phlorizin and sodium on glucose-elicited alterations of cell junctions in intestinal epithelia. *Am J Physiol*, 1990, **258**, C77-85.